UMTA-MA-06-0025-77-18

# EXCITATION OF SURFACE ELECTROMAGNETIC WAVES ON RAILROAD RAIL

C.A. Goben
M. Davarpanah

University of Missouri-Rolla
Rolla MO 65401



MARCH 1978

FINAL REPORT



Prepared for
U.S DEPARTMENT OF TRANSPORTATION
URBAN MASS TRANSPORTATION ADMINISTRATION
Office of Technology Development and Deployment
Office of Rail Technology
Washington DC 20590

NOTICE

This document is disseminated under the sponsorship of the Department of Transportation in the interest of information exchange. The United States Government assumes no liability for its contents or use thereof.



NOTICE

The United States Government does not endorse products or manufacturers. Trade or manufacturers' names appear herein solely because they are considered essential to the object of this report.

Technical Report Documentation Page

| 1. Report No. | 2. Government Accession No. | 3. Recipient's Catalog No |
|---|---|---|
| UMTA-MA-06-0025-77-18 | | |

| 4. Title and Subtitle | 5. Report Date |
|---|---|
| EXCITATION OF SURFACE ELECTROMAGNETIC WAVES ON RAILROAD RAIL | March 1978 |
| | 6. Performing Organization Code |
| | 8. Performing Organization Report No. |
| 7. Author(s) | DOT-TSC-UMTA-76-19 |
| C.A. Goben and M. Davarpanah | |
| 9. Performing Organization Name and Address | 10. Work Unit No. (TRAIS) |
| University of Missouri-Rolla*<br>Rolla MO 65401 | UM804/R8723 |
| | 11. Contract or Grant No. |
| | DOT-TSC-1150 |
| 12. Sponsoring Agency Name and Address | 13. Type of Report and Period Covered |
| U.S. Department of Transportation<br>Urban Mass Transportation Administration<br>Office of Technology Development and Deployment<br>Office of Rail Technology<br>Washington DC 20590 | Final Report<br>January 1976-July 1976 |
| | 14. Sponsoring Agency Code |

15. Supplementary Notes

*Under contract to: U.S. Department of Transportation
Transportation Systems Center
Kendall Square
Cambridge MA 02142



16. Abstract

Surface Electromagnetic Waves (SEW) have been successfully propagated on the surface of standard railroad rail and other metallic surfaces. Preliminary investigation of the propagation properties of SEW on rail surfaces indicates that there exist applications in train-and-obstacle detection. The excitation efficiences of two types of SEW Couplers (Prism and Grating) when in the vicinity of the rail are measured as functions of frequency, vertical displacement (h) of the coupler above the rail, horizontal (lateral) displacement (a) of the coupler from rail center, pitch angle (Phi) of the coupler, roll angle (Theta) of the coupler, and yaw angle (Psi) of the coupler. The coupling efficiencies for both prism-and-grating couplers show a dependence on vertical displacement above the rail; horizontal displacement from rail center, and pitch, roll, and yaw angles of the couplers. Measurements of radiation patterns have also been made on the two types of SEW couplers in the vicinity of the rail and in isolation at several microwave frequencies. The results of radiation-pattern data show that to meet the FCC specification of 500 μV/m at 100 ft from the coupler for 100 mW input, the couplers be redesigned. Redesigning the couplers involves the use of absorbing material around the couplers to reduce the radiating power in the non-transmitting directions which exceeds the FCC limits. The data indicate that both the prism coupler and grating coupler will operate successfully on a moving track-guided vehicle.

| 17. Key Words | 18. Distribution Statement |
|---|---|
| Non-Contact Couplers<br>Railway Collision Avoidance<br>Surface Electromagnetic Waves<br>Prism Coupler, Grating Coupler | DOCUMENT IS AVAILABLE TO THE PUBLIC THROUGH THE NATIONAL TECHNICAL INFORMATION SERVICE, SPRINGFIELD, VIRGINIA 22161 |

| 19. Security Classif. (of this report) | 20. Security Classif. (of this page) | 21. No. of Pages | 22. Price |
|---|---|---|---|
| Unclassified | Unclassified | 64 | |

Form DOT F 1700.7 (8-72) Reproduction of completed page authorized

# PREFACE

The Office of Rail Technology of the Urban Mass Transportation Administration (UMTA) has been conducting research and development programs directed toward the improvement of urban rail transportation systems safety.

One type of accident which occurs from time to time is rear-end train collision even in track sections with signal systems.

As a result, rail-transit research seeks to develop an on-board, separate and independent obstacle-dection system, so that rear-end collisions can be avoided.

One possible system involves the use of Surface Electromagnetic Wave (SEW) detection. The aim of the work performed under this contract is to determine the feasibility of such a system in a rail-transit operation.

The authors wish to thank R. Kodis and P. Yoh of the Transportation Systems Center (TSC) for helpful discussions and for useful suggestions.

## METRIC CONVERSION FACTORS

### Approximate Conversions to Metric Measures

| Symbol | When You Know | Multiply by | To Find | Symbol |
|---|---|---|---|---|
| | **LENGTH** | | | |
| in | inches | 2.5 | centimeters | cm |
| ft | feet | 30 | centimeters | cm |
| yd | yards | 0.9 | meters | m |
| mi | miles | 1.6 | kilometers | km |
| | **AREA** | | | |
| $in^2$ | square inches | 6.5 | square centimeters | $cm^2$ |
| $ft^2$ | square feet | 0.09 | square meters | $m^2$ |
| $yd^2$ | square yards | 0.8 | square meters | $m^2$ |
| $mi^2$ | square miles | 2.6 | square kilometers | $km^2$ |
| | acres | 0.4 | hectares | ha |
| | **MASS (weight)** | | | |
| oz | ounces | 28 | grams | g |
| lb | pounds | 0.45 | kilograms | kg |
| | short tons (2000 lb) | 0.9 | tonnes | t |
| | **VOLUME** | | | |
| tsp | teaspoons | 5 | milliliters | ml |
| Tbsp | tablespoons | 15 | milliliters | ml |
| fl oz | fluid ounces | 30 | milliliters | ml |
| c | cups | 0.24 | liters | l |
| pt | pints | 0.47 | liters | l |
| qt | quarts | 0.95 | liters | l |
| gal | gallons | 3.8 | liters | l |
| $ft^3$ | cubic feet | 0.03 | cubic meters | $m^3$ |
| $yd^3$ | cubic yards | 0.76 | cubic meters | $m^3$ |
| | **TEMPERATURE (exact)** | | | |
| °F | Fahrenheit temperature | 5/9 (after subtracting 32) | Celsius temperature | °C |

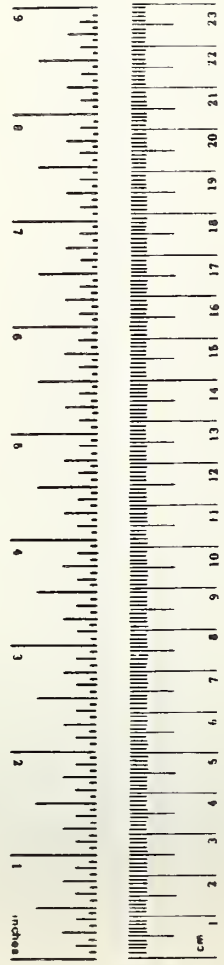


### Approximate Conversions from Metric Measures

| Symbol | When You Know | Multiply by | To Find | Symbol |
|---|---|---|---|---|
| | **LENGTH** | | | |
| mm | millimeters | 0.04 | inches | in |
| cm | centimeters | 0.4 | inches | in |
| m | meters | 3.3 | feet | ft |
| m | meters | 1.1 | yards | yd |
| km | kilometers | 0.6 | miles | mi |
| | **AREA** | | | |
| $cm^2$ | square centimeters | 0.16 | square inches | $in^2$ |
| $m^2$ | square meters | 1.2 | square yards | $yd^2$ |
| $km^2$ | square kilometers | 0.4 | square miles | $mi^2$ |
| ha | hectares (10,000 $m^2$) | 2.5 | acres | |
| | **MASS (weight)** | | | |
| g | grams | 0.035 | ounces | oz |
| kg | kilograms | 2.2 | pounds | lb |
| t | tonnes (1000 kg) | 1.1 | short tons | |
| | **VOLUME** | | | |
| ml | milliliters | 0.03 | fluid ounces | fl oz |
| l | liters | 2.1 | pints | pt |
| l | liters | 1.06 | quarts | qt |
| l | liters | 0.26 | gallons | gal |
| $m^3$ | cubic meters | 35 | cubic feet | $ft^3$ |
| $m^3$ | cubic meters | 1.3 | cubic yards | $yd^3$ |
| | **TEMPERATURE (exact)** | | | |
| °C | Celsius temperature | 9/5 (then add 32) | Fahrenheit temperature | °F |

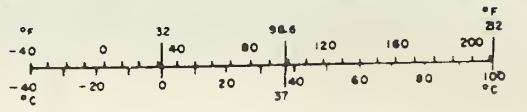

CONTENTS

ILLUSTRATIONS

ILLUSTRATIONS (Cont'd)

ILLUSTRATIONS (CONCL'D)

# 1. INTRODUCTION

The use of surface electromagnetic waves (SEW) for communication, control, obstacle detection, and fault detection on guided railroad systems is already being considered in several countries; for example, the United States,[1-4] United Kingdom,[5-7] Japan,[8-12] and Canada.[13-19] One of the major applications of SEW in railway systems is the detection of trains and obstacles on the track. This function is important to system safety, especially on high-speed railways or guideways. Our preliminary investigations[20,21] with SEW propagating on the top of railraod rails indicate that train or obstacle detection is possible using SEW.

A coupler having no physical contact with the rail is required to excite and detect SEW from the train. We report here the measurements of the coupling efficiences for two types of SEW couplers (prism and grating) as functions of frequency, vertical displacement of the coupler above the rail, horizontal (lateral) displacement of the coupler from rail center; pitch, roll, and yaw angles of the coupler. Radiation patterns have also been measured on the two types of SEW couplers in the vicinity of the rail and in isolation at several microwave frequencies.

The coupling efficiency is defined[2-23] as the ratio of the power carried by the SEW along the surface to the power transmitted through the coupling aperture and available for coupling to the SEW. The coupling aperture (coupling area) is the effective cross-sectional area of the prism or the grating, which interacts with the railroad rail surface and which can act to couple power to the SEW (see Appendix III of Ref. 23). The dependence of the coupling aperture on the SEW excitation technique is also discussed in Appendix III of Ref. 23.

# 2. BACKGROUND

## 2.1 SURFACE ELECTROMAGNETIC WAVES

SEW has been defined by Barlow and Brown:[22]

"A SURFACE WAVE IS ONE THAT PROPAGATES ALONG AN INTERFACE BETWEEN TWO DIFFERENT MEDIA WITHOUT RADIATION; SUCH RADIATION BEING CONSTRUED TO MEAN ENERGY CONVERTED FROM THE SURFACE-WAVE FIELD TO SOME OTHER FORM."

From this definition, it is seen that the most distinctive property of SEW is the non radiating property as it propagates along an interface. This, in addition to the need of only one conductor as a transmission line, will make SEW potentially very useful in fault detection systems, collision avoidance systems, and communications systems.[24-26]

Although there are three distinctive forms of SEW, this work is concerned with inhomogeneous plane waves supported by a flat conducting surface (Zenneck Waves). A bare railroad rail (iron) is used for the supporting medium. The medium above the metal is air.

## 2.2 SURFACE ELECTROMAGNETIC WAVE FIELDS

SEW which are guided along an uncoated metallic conductor are represented by particular solution of Maxwell's equations. It is assumed that the conducting boundary is in the x-y plane and that there is variation in the x-direction is no variation in the y-direction ($\partial/\partial y = 0$). It is also assumed that the SEW is a transverse magnetic wave (TM); therefore, there are only three field components, $E_x$, $E_z$, and $H_y$, in each medium.

Wave solutions are required in two half-spaces as indicated in Fig. 1. Air is represented by Region 1 and the conductor by Region 2. The expressions

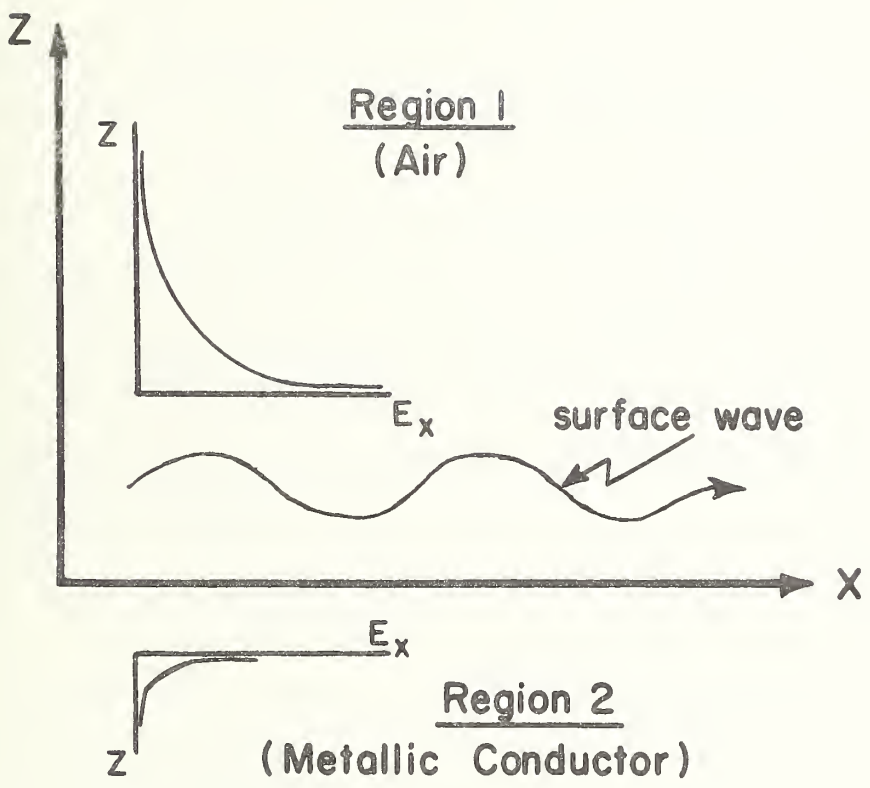


FIGURE 1. SURFACE ELECTROMAGNETIC WAVE IS GUIDED ALONG METALLIC PLANE.

for field components are as follows:[23]

Air-Region 1 (z>o)

$$Hy = A \exp(-k_{z_1} z) \exp(-j(k_x x - \omega t)),$$
$$Ex = A \frac{k_{z_1}}{j\omega\epsilon_1} \exp(-k_{z_1} z) \exp(-j(k_x x - \omega t)), \quad (1)$$
$$E_z = -A \frac{kx}{\omega\epsilon_1} \exp(-k_{z_1} z) \exp(-j(k_x x - \omega t)).$$

Metallic Conductor-Region 2(z< o)

$$Hy = A \exp(k_{z_2} z) \exp(-j(k_x x - \omega t)),$$
$$Ex = A \frac{k_{z_2}}{j\omega\epsilon_{2eff}} \exp(k_{z_2} z) \exp(-j(k_x x - \omega t)), \quad (2)$$
$$E_z = -A \frac{k_x}{\omega\epsilon_{2eff}} \exp(k_{z_2} z) \exp(-j(k_x x - \omega t)),$$

where $k_x$ and $k_z$ are the propagation vectors in the x-and-z directions, respectively. The subscripts 1 and 2 refer to Regions 1 (air) and 2 (conductor). The dispersion relation is given by[23]

$$k_x = \frac{\omega}{c} \sqrt{\frac{\epsilon_{2eff}(\epsilon_1/\epsilon_0)}{\epsilon_{2eff} + \epsilon_1}}, \quad (3)$$

where $\epsilon_1$ is the permittivity of air, $\epsilon_0$ is the permittivity of free space, $\omega$ is the SEW angular frequency, c is the speed of light in free space, and

$$\epsilon_{2eff} = \epsilon_2 - j\frac{\sigma_2}{\omega}, \quad (4)$$

where $\epsilon_2$ and $\sigma_2$ are the total permittivity and conductivity of the metal, respectively. For metal conductors in the microwave region, to a good approximation:

$$\frac{\sigma_2}{\omega} >> |\epsilon_2| .$$

Therefore, Eq. (4) becomes

$$\varepsilon_{2eff} \simeq -j\frac{\sigma_2}{\omega} . \tag{5}$$

Substituting Eq. (5) into Eq. (3) and noting that $\frac{\sigma_2}{\omega} >> \varepsilon_1$ and that $\varepsilon_1 \simeq \varepsilon_0$, we find that the propagation constant in the x-direction is approximately

$$k_x = \frac{\omega}{c} . \tag{6}$$

Therefore, for the efficient excitation of SEW on an uncoated conducting surface at microwave frequencies, the magnitude of the propagation vector will be w/c, the free-space value.

The fields decay outside of the surface exponentially. The component of the propagation vector in the +z-direction (air) is[23]

$$k_{z_1} = \frac{\omega}{c} \frac{\varepsilon_1}{\varepsilon_0} \sqrt{\frac{-\varepsilon_0}{\varepsilon_{2eff} + \varepsilon_1}} . \tag{7}$$

The component of propagation vector in the -z direction (metallic conductor) is[23]

$$k_{z_2} = -\frac{\omega}{c} \frac{\varepsilon_{2eff}}{\varepsilon_0} \sqrt{\frac{-\varepsilon_0}{\varepsilon_{2eff} + \varepsilon_1}} . \tag{8}$$

The fields fall to $\frac{1}{e}$ of their surface value at a height[23]

$$h_{air} = \frac{1}{Re\ (k_{z_1})} , \tag{9}$$

$$h_{metal} = \frac{1}{Re\ (k_{z_2})} , \tag{10}$$

The height above the surface for 90-percent power concentration is[23]

$$h_{90\%} = 2.3 \frac{c}{\omega} \sqrt{\sigma_2 / 2\omega\varepsilon_0'} , \tag{11}$$

## 2.3 SURFACE ELECTROMAGNETIC WAVE EXCITATION TECHNIQUES

All previously employed methods of SEW excitation have required physical contact between the metallic surface (guiding structure) connected to the

coupling aperture. Our use of the prism or grating coupler allows the excitation of SEW without any physical contact between the coupler and metallic conductor (railroad rail). The prism-and-grating coupling techniques for SEW excitation will now be considered subject to the approximation that $k_x$ is equal to $\omega/c$.

2.3.1 Prism-coupling Technique

If a metal surface, coated or uncoated, is brought under a dielectric prism maintaining a small air gap (of the order of a wavelength) between the base of the prism and the conducting surface, SEW can be excited on the conducting surface. Fig. 2(a) illustrates the principle of the prism coupling technique.[27-31] For this situation, an evanescent wave is propagating along the surface. The x-component of the propagation vector of this evanescent wave is [20,21]

$$k_x = \varepsilon_d \, (\omega/c) \sin \theta_i . \tag{12}$$

Using the approximation that $k_x$ is equal to $\omega/c$ in Eq. (12) results in

$$\sin \theta_i = \frac{1}{\sqrt{\varepsilon_d}} = \frac{1}{n} , \tag{13}$$

where n is the index refraction of the prism coupler. Therefore, to excite SEW by prism coupler, $\theta_1$ will be equal to the critical angle $\theta_c$ of the prism coupler (see Fig. 2).

To couple SEW onto metal surfaces and to decouple at the receiving point, right-angle prisms are used, as shown in Fig. 2(b). A maximum coupling efficiency of 60 percent has been achieved experimentally for prism-coupling technique.[20,21,23]

2.3.2 Grating-coupling Technique

A grating coupler for the excitation of SEW is shown schematically in

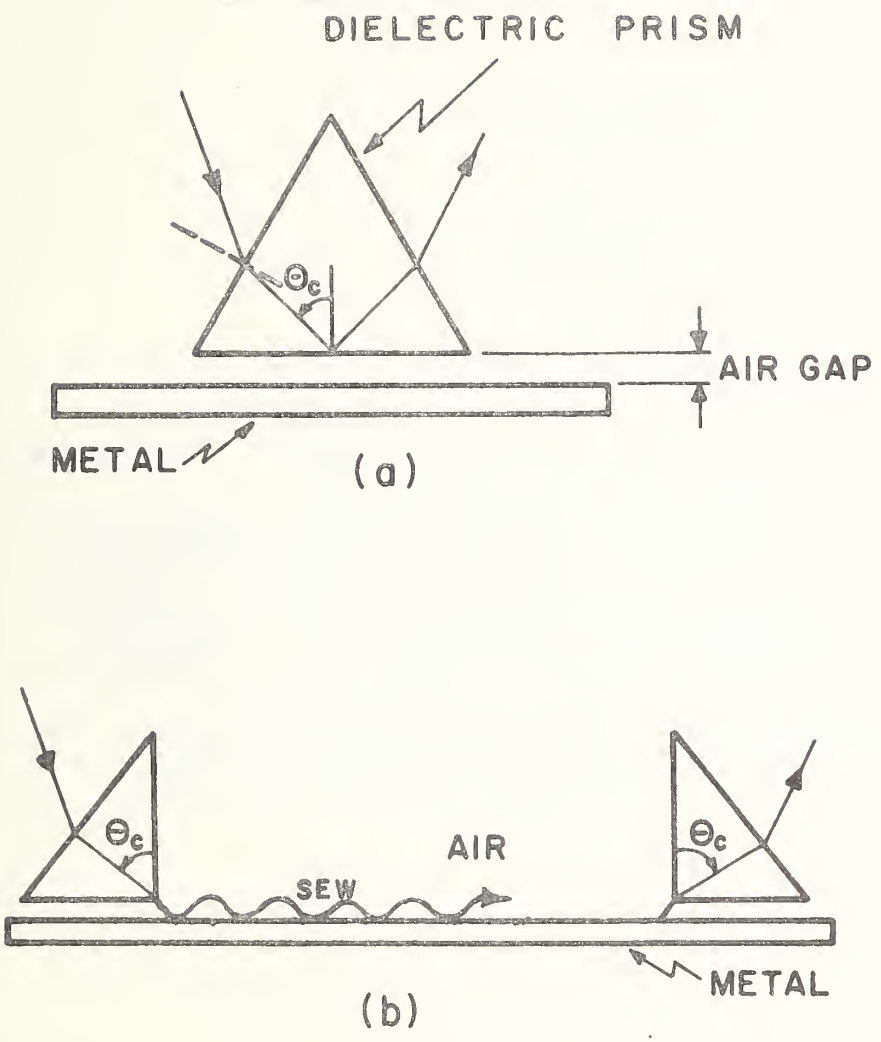


FIGURE 2. (a) PRISM-COUPLING TECHNIQUE PRINCIPLE SHOWING CRITICAL ANGLE ($\theta c$), (b) COUPLING IN AND OUT OF SURFACE ELECTROMAGNETIC WAVES BY PRISM COUPLERS.

Fig. 3. It excites waves with propagation vector corresponding to the set[27]

$$k_x = (\omega/c)\sin\alpha + m\frac{2\pi}{d} \quad m = 0, \pm 1, \pm 2, \ldots , \tag{14}$$

where

$\alpha$ = the angle of incidence,

m = mode order, and

d = grating constant.

In the microwave region $k_x = \omega/c$, and Eq. (14) yields

$$\sin\alpha = 1 - m\frac{\lambda}{d} \quad m = 0, \pm 1, \pm 2, \tag{15}$$

where $\lambda$ is the wavelength of SEW. Therefore, to excite SEW with the grating coupler, the angle of incidence $\alpha$ must satisfy Eq. 15. A maximum coupling efficiency of 30 percent has been achieved experimentally for the grating-coupling technique with m = 1.

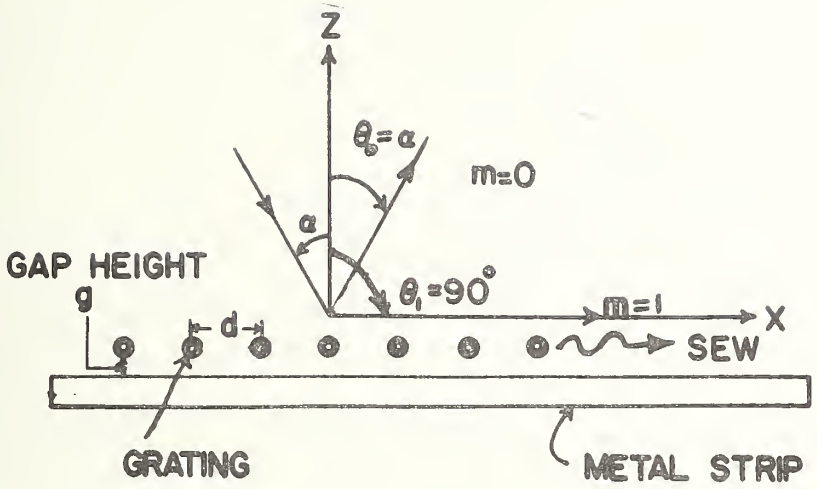


FIGURE 3. GRATING-COUPLING TECHNIQUE PRINCIPLE SHOWING ANGLE OF INCIDENCE ($\alpha$), GRATING SPACING (d), AND GAP HEIGHT (g). MODE ORDER 1 IS SHOWN COUPLED AS SEW ($\theta = 90^\circ$).

## 3. SURFACE ELECTROMAGNETIC WAVE COUPLING EFFICIENCY

The efficiency of each coupler has been measured as functions of frequency, vertical displacement (h) of the coupler above the rail, horizontal (lateral) displacement (a) of the coupler from rail center; and pitch, roll, and yaw angles of the coupler.

The measuring techniques are described below. All signal readings are normalized for plotting to the maximum signal being delivered to the coupler aperture. SEW signal strengths are measured as described in the following sections.

### 3.1 COUPLING EFFICIENCY VS VERTICAL DISPLACEMENT

The prism-coupler excitation efficiencies as functions of the (vertical displacement)/(wavelength) for the soft polyethylene prism coupler have been measured at 8.2 and 16 GHz and are plotted in Figs. 4 and 5, respectively. The vertical displacement (h) is varied from 0 to 3 wavelengths in 0.2-wavelength steps for 8.2 and 16 GHz (see Fig. 6a). A horn antenna is used in this experiment to receive the SEW signals. The data show that the peak in excitation efficiency for the prism-coupling technique occurs in one-half-wavelength vertical displacement above the rail. The maximum prism coupling efficiencies are 57 and 60 percent at 8.2 and 16 GHz, respectively.

The grating coupling efficiencies have been as functions of the (vertical displacement)/(wavelength) at 8 and 12 GHz, and are plotted in Figs. 7 and 8, respectively. The coupling efficiencies peak every 1/2-wavelength in vertical displacement. The maximum grating-coupling efficiencies measured are 26 percent at 8 GGz and 30 percent at 12 GHZ.

The changes in efficiency with respect to vertical displacement in a normal-size track-guided vehicle will be small since the vertical displacement expected in normal operation is only a few centimeters.

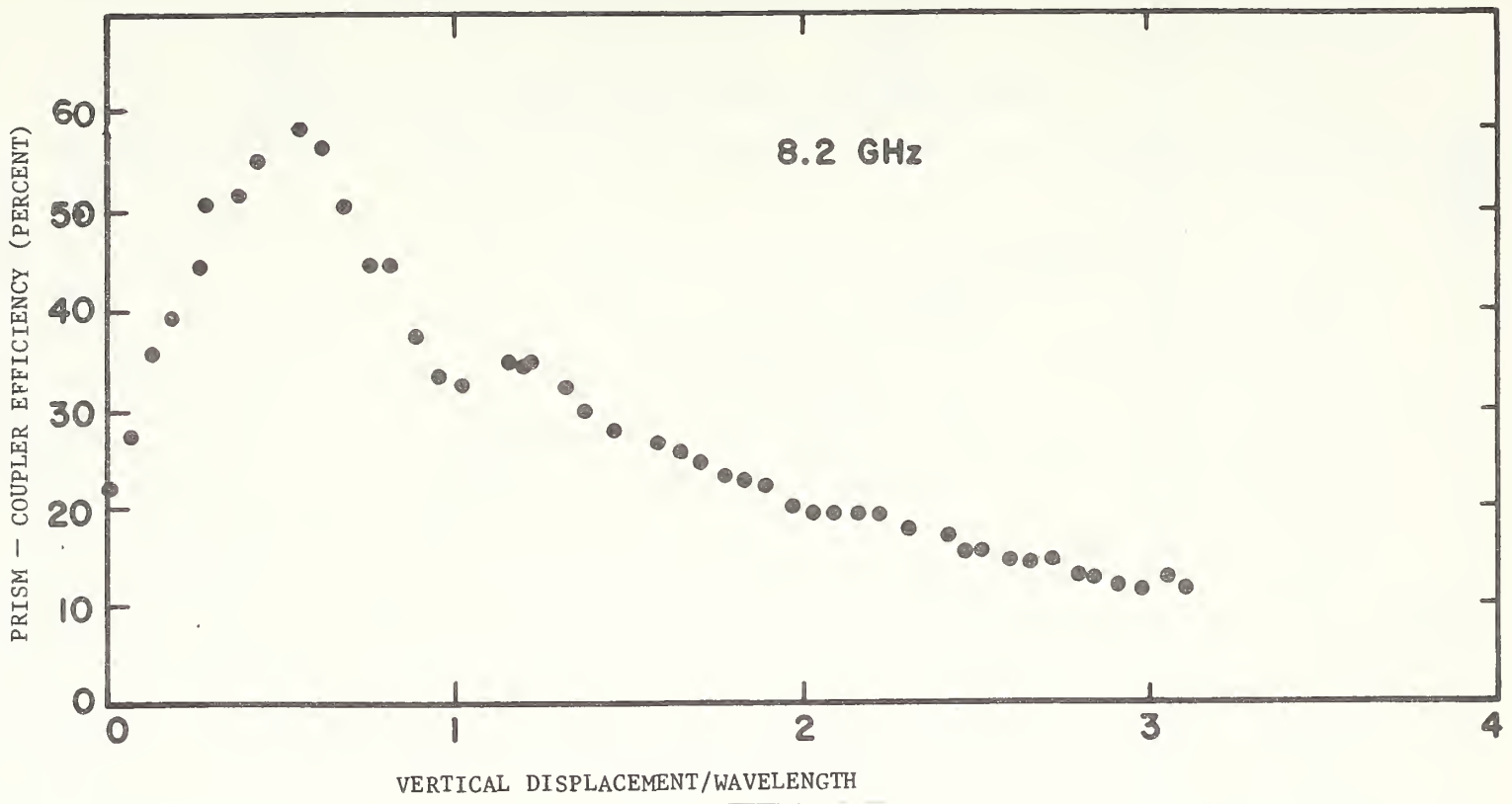


FIGURE 4 PRISM-COUPLER EXCITATION EFFICIENCY VS (VERTICAL DISPLACEMENT/(WAVELENGTH) ON STANDARD RAILROAD RAIL AT 8.2 GHz.

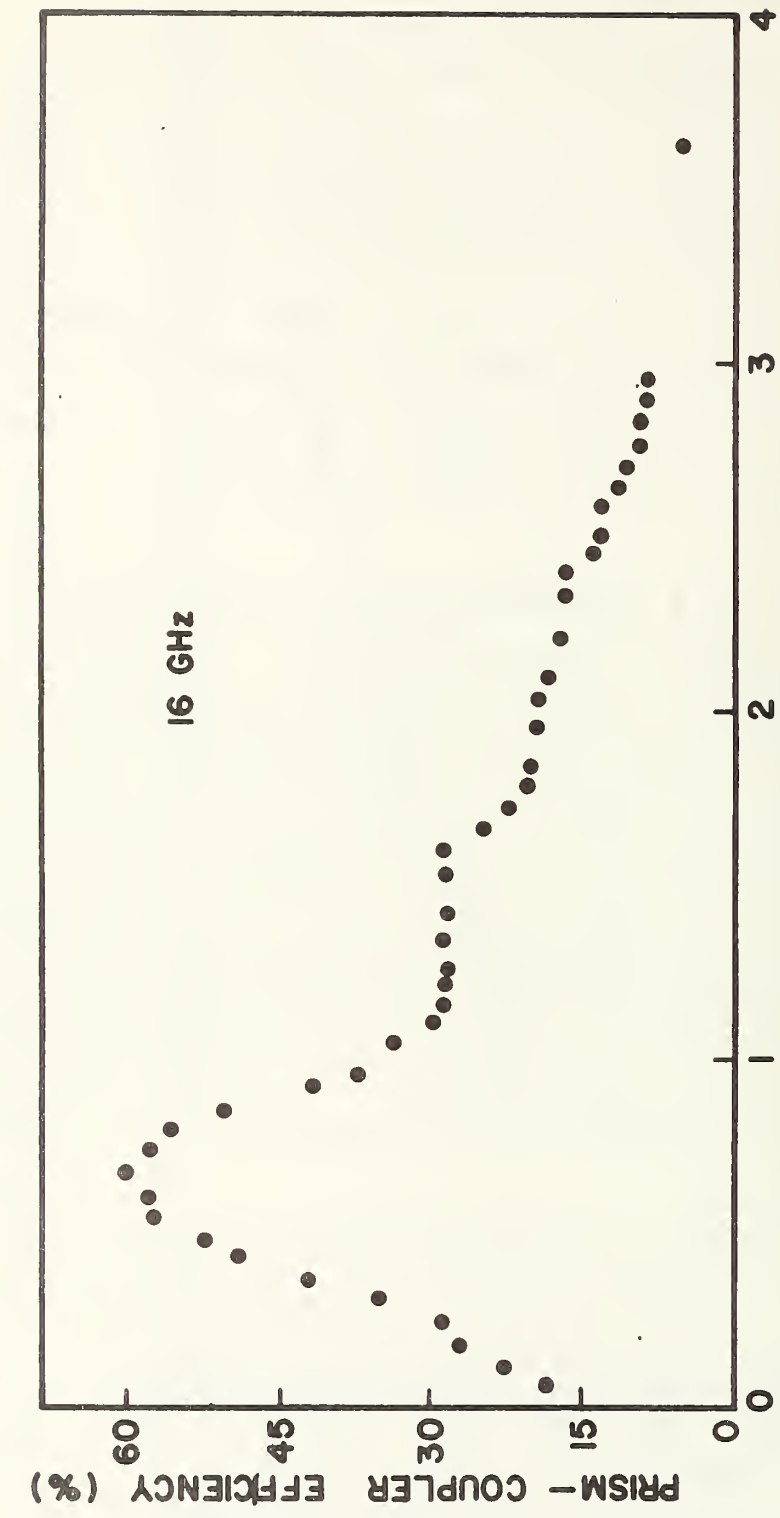


FIGURE 5 PRISM-COUPLER EXCITATION EFFICIENCY VS (VERTICAL DISPLACEMENT)/(WAVELENGTH) ON STANDARD RAILROAD RAIL AT 16 GHz.

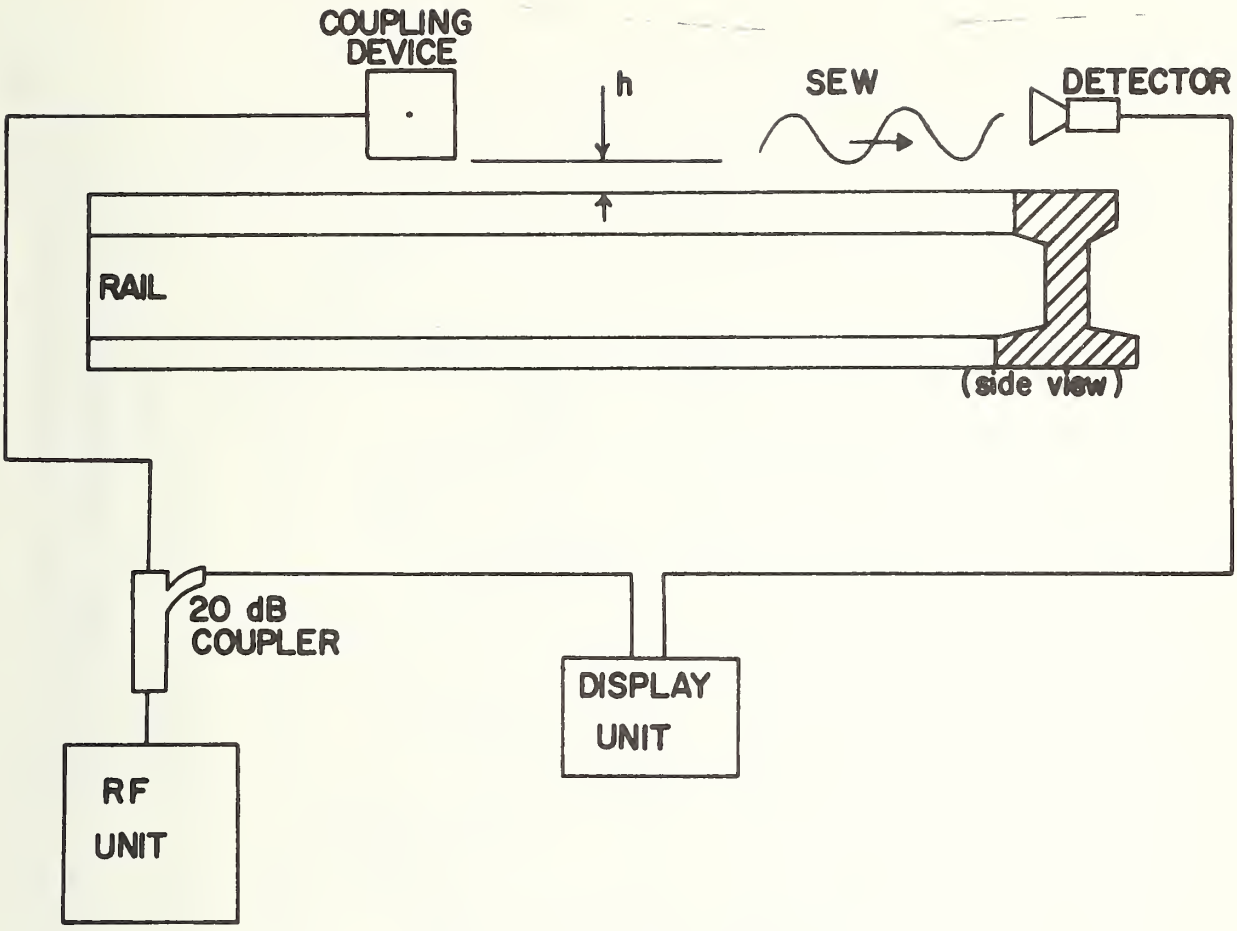


FIGURE 6a. VERTICAL DISPLACEMENT (h) MEASUREMENT.

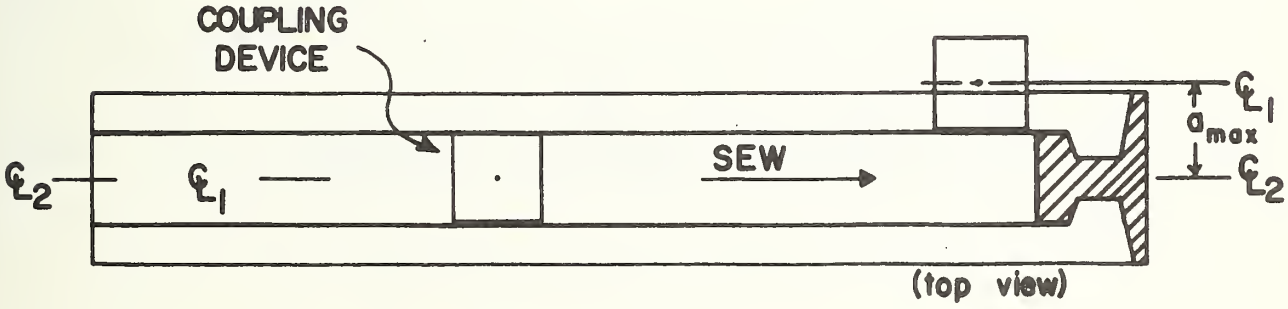


FIGURE 6b. HORIZONTAL (LATERAL) DISPLACEMENT (a) MEASUREMENT.

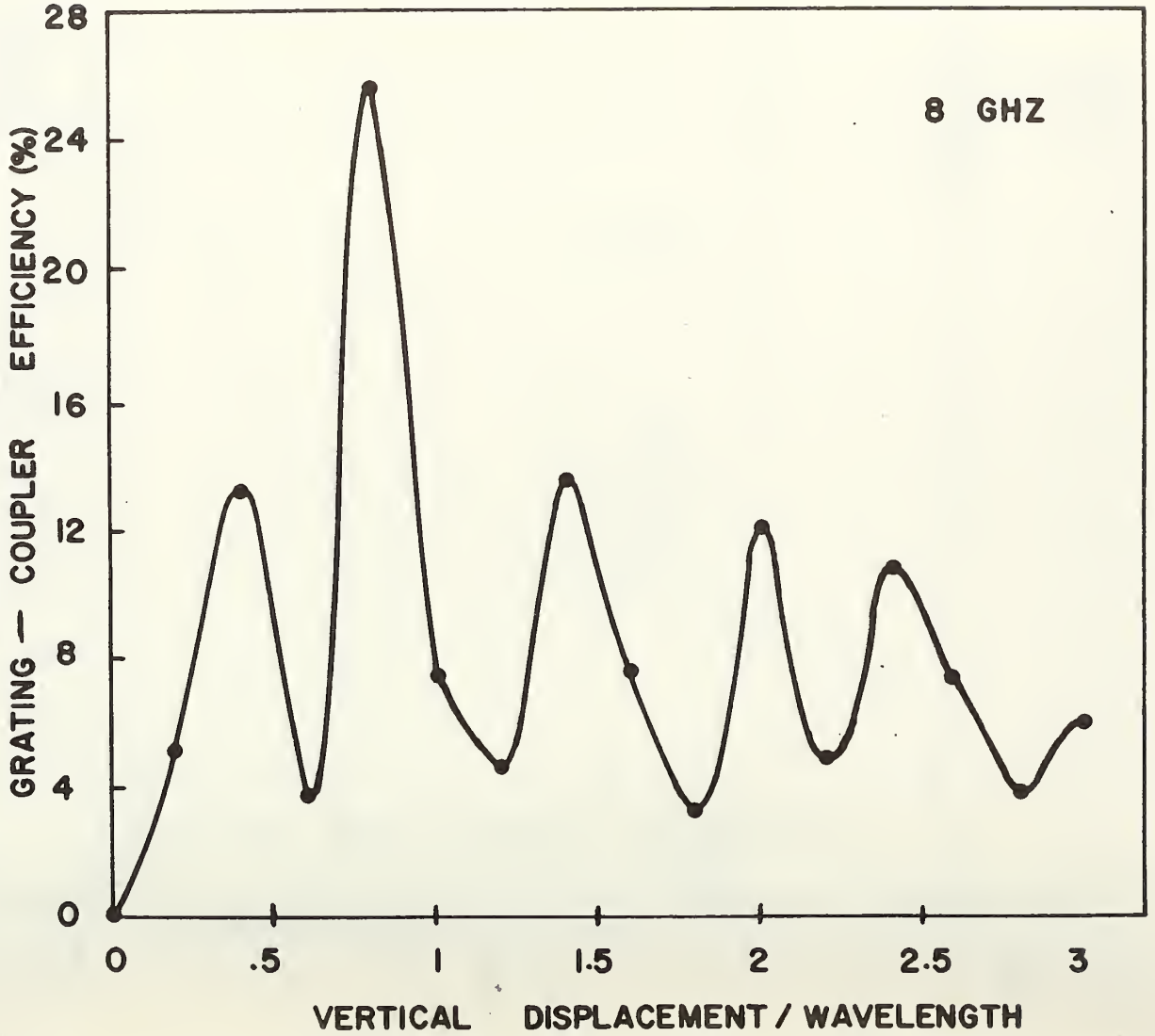


FIGURE 7. GRATING-COUPLER EXCITATION EFFICIENCY VS (VERTICAL DISPLACEMENT)/(WAVELENGTH) ON STANDARD RAILROAD RAIL AT 8 GHz.

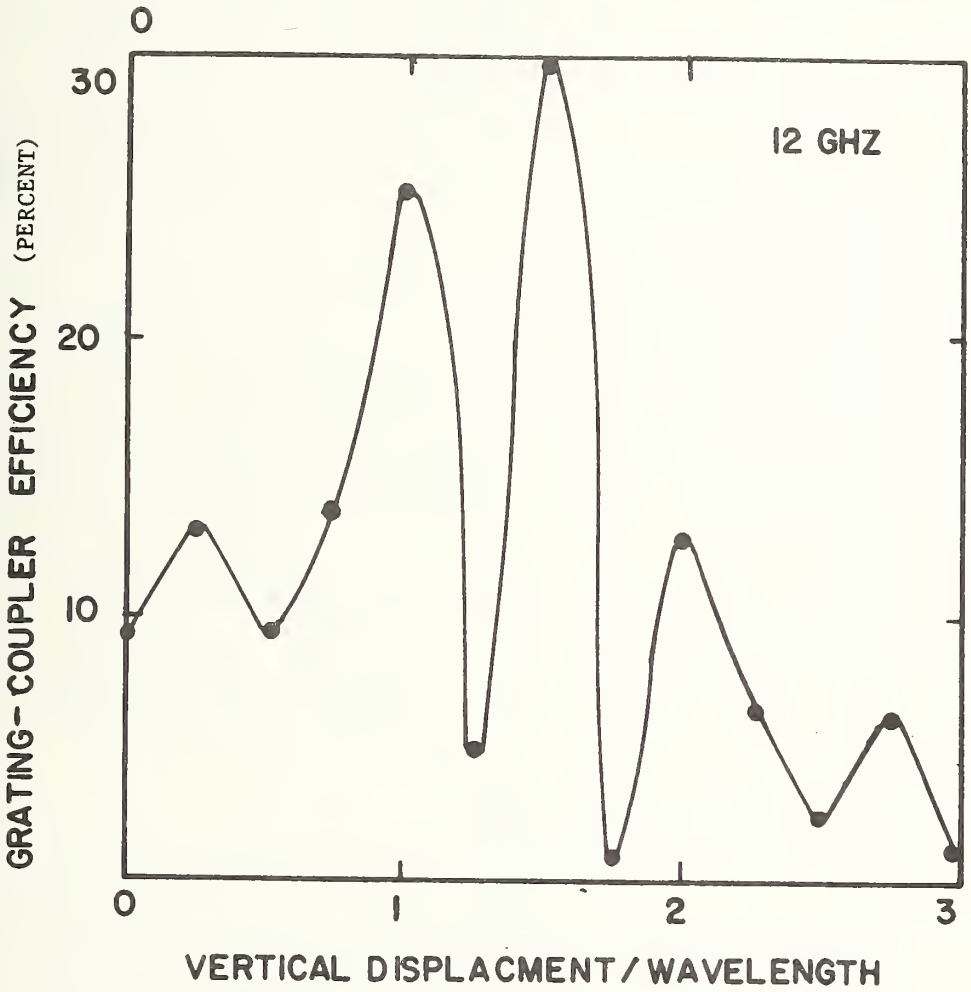


FIGURE 8. GRATING-COUPLING EXCITATION EFFICIENCY VS (VERTICAL DISPLACEMENT/WAVELENGTH) ON STANDARD RAILROAD RAIL AT 12 GHz.

## 3.2 COUPLING EFFICIENCY VS HORIZONTAL DISPLACEMENT

The maximum prism-coupling efficiencies of 57 and 60 percent have been achieved with the prism near the center of the rail at 8.2 and 16 GHz, respectively (see Figs. 9, 10). The efficiency falls off asymmetrically for 8.2 GHz and more asymmetrically for 16 GHz as the coupler is displaced from the rail center to the maximum displacement (as shown in Fig. 6b), $a_{max}$ = (rail width/2) + (coupler width/2). The asymmetry in the data is attributed to the rail being asymmetrical because of wear, and this effect is relatively more pronounced when the ratio of the wavelength to the rail dimension is smaller.

The maximum grating-coupling efficiencies of 26 and 30 percent have been achieved with grating near the center of the rail at 8 and 12 GHz, respectively (see Figs. 11, 12). The efficiencies fall off asymmetrically for both frequencies. The asymmetry in the data is attributed to the rail being asymmetrical.

The change in efficiency with respect to horizontal displacment in a normal-size track-guided vehicle will be small since the horizontal displacement expected in normal operation is only a few centimeters.

## 3.3 COUPLING EFFICIENCY VS PITCH ANGLE

Prism-coupling efficiencies as functions of pitch angles are shown in Figs. 13 and 14 for 8.2 and 16 GHz, respectively. The pitch angle (Phi) is varied in 0.2-degree increments for 0 to ± 2 degrees and 0.5-degree increments from ± 2 to 5 degrees at the optimum vertical displacement determined in 3.1 (see Fig. 15a).

Notice that there is an increase in coupling efficiency when the prism coupler is rotating in the positive-angle direction. The prism is designed to couple more efficiently when a parallel beam enters it perpendicularly to the back face of the prism (see Fig. 16a), When this condition is met, the beam

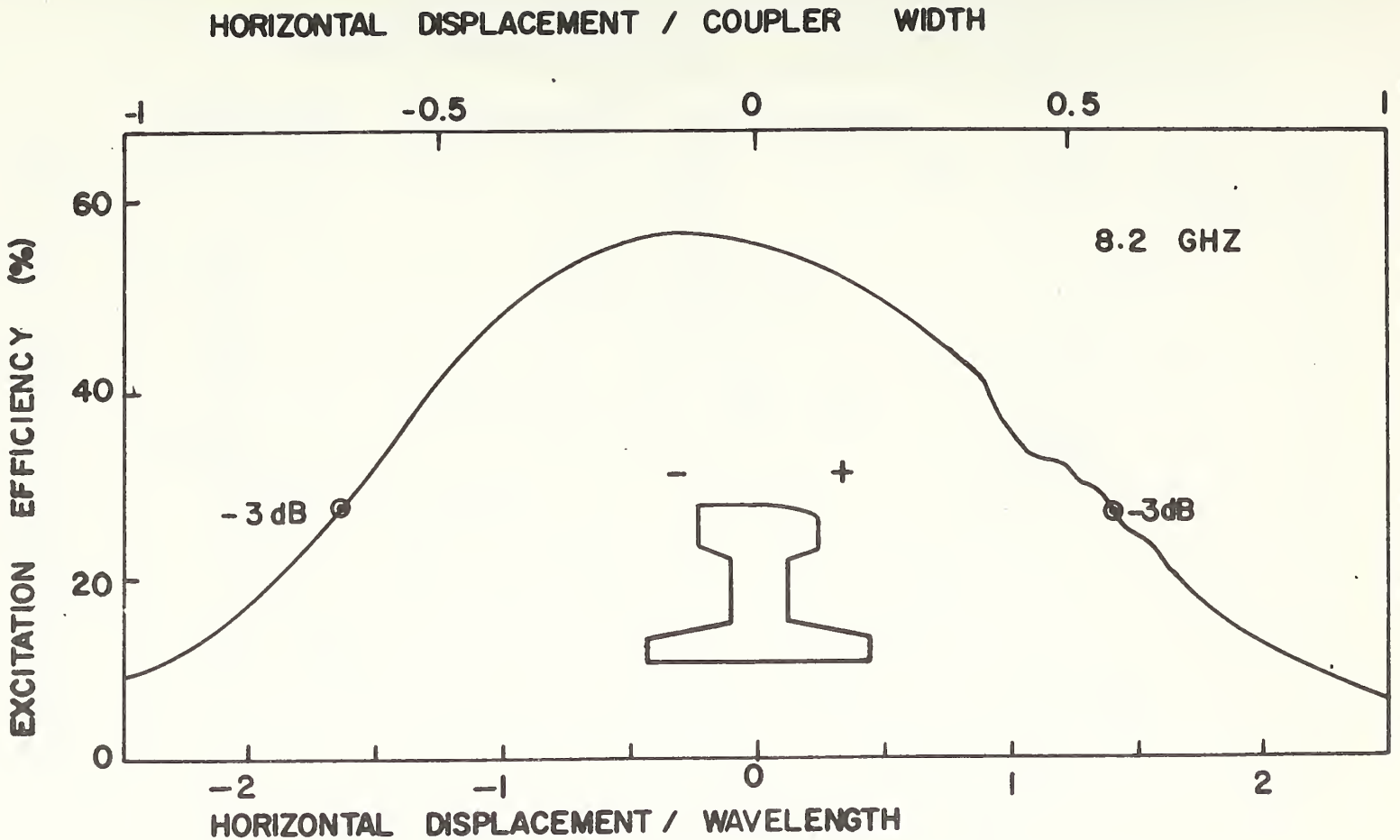


FIGURE 9. PRISM-COUPLER EXCITATION EFFICIENCY VS (HORIZONTAL DISPLACEMENT)/(WAVELENGTH) ON STANDARD RAILROAD RAIL AT 8.2 GHz.

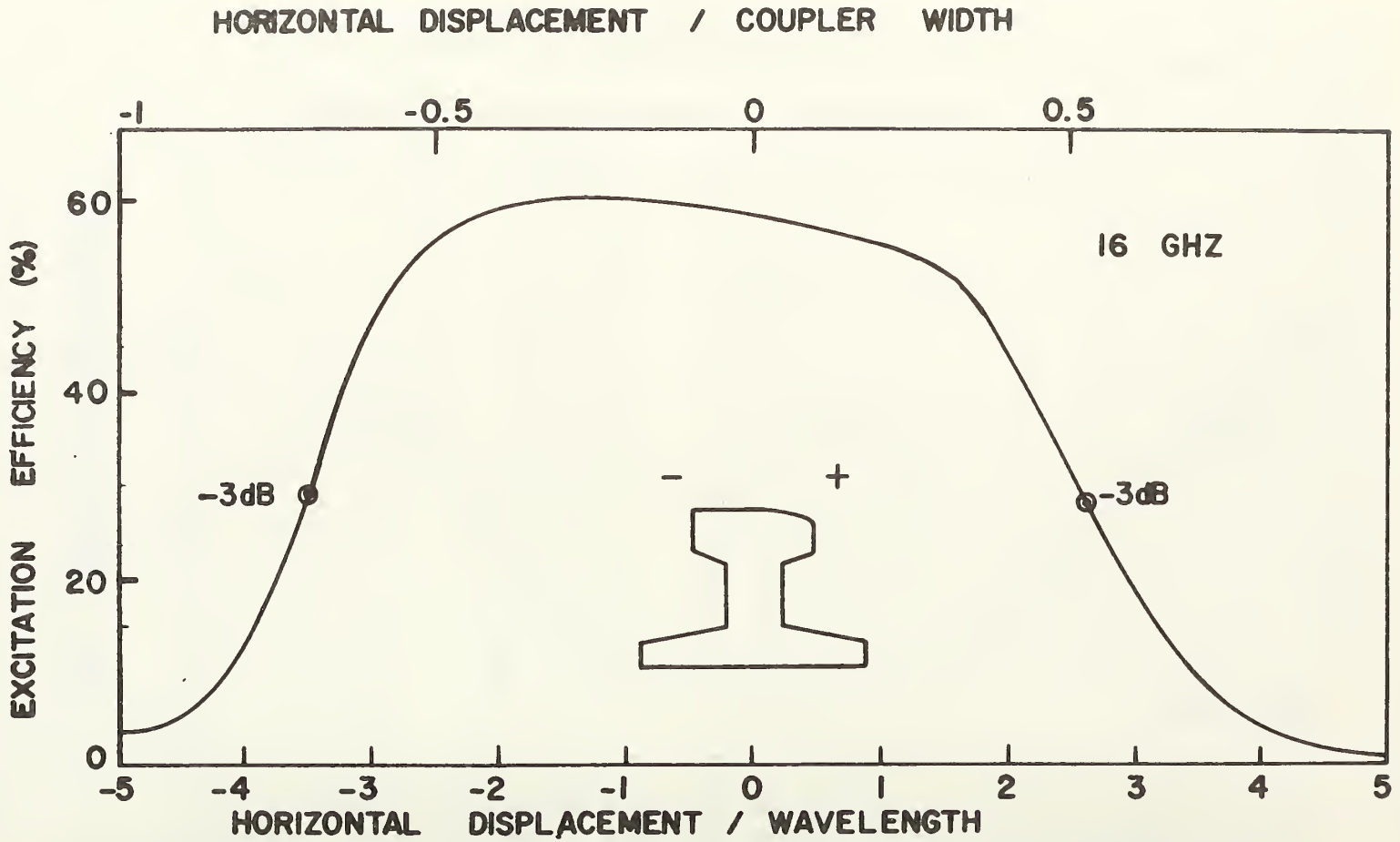


FIGURE 10. PRISM-COUPLER EXCITATION EFFICIENCY VS (HORIZONTAL DISPLACEMENT)/(WAVELENGTH) ON STANDARD RAILROAD RAIL AT 16 GHz.

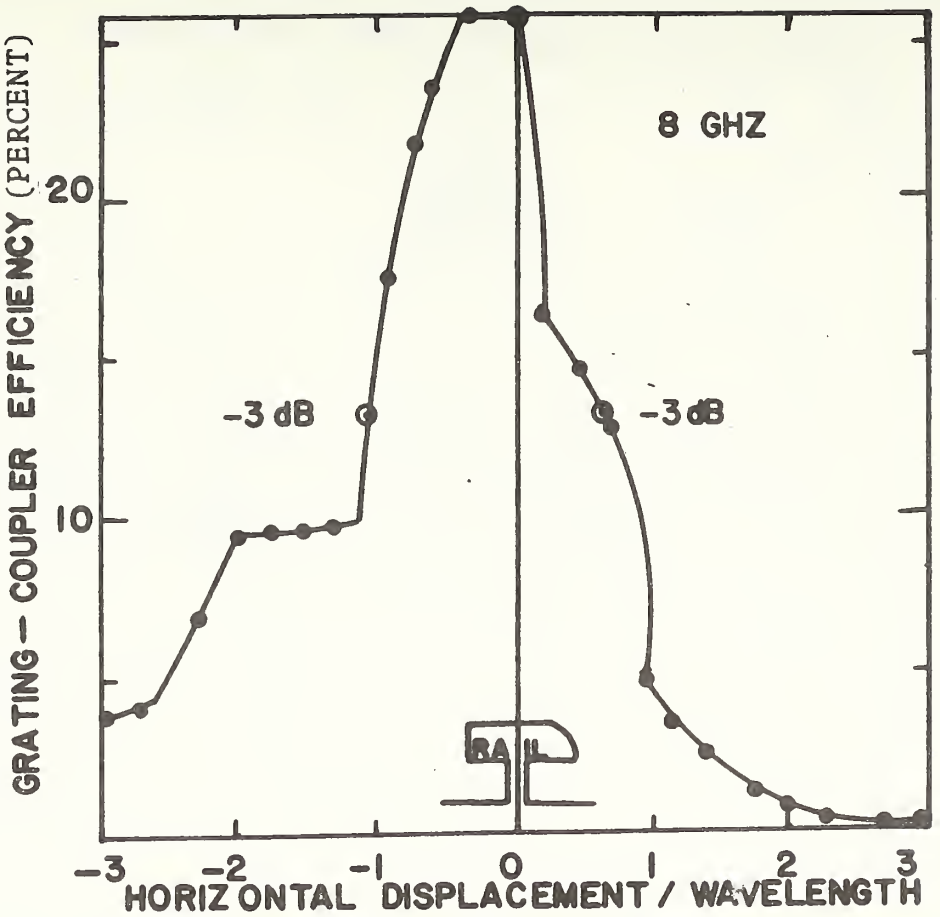


FIGURE 11. GRATING-COUPLER EXCITATION EFFICIENCY VS (HORIZONTAL DISPLACEMENT)/ (WAVELENGTH) ON STANDARD RAILROAD RAIL AT 8 GHz.

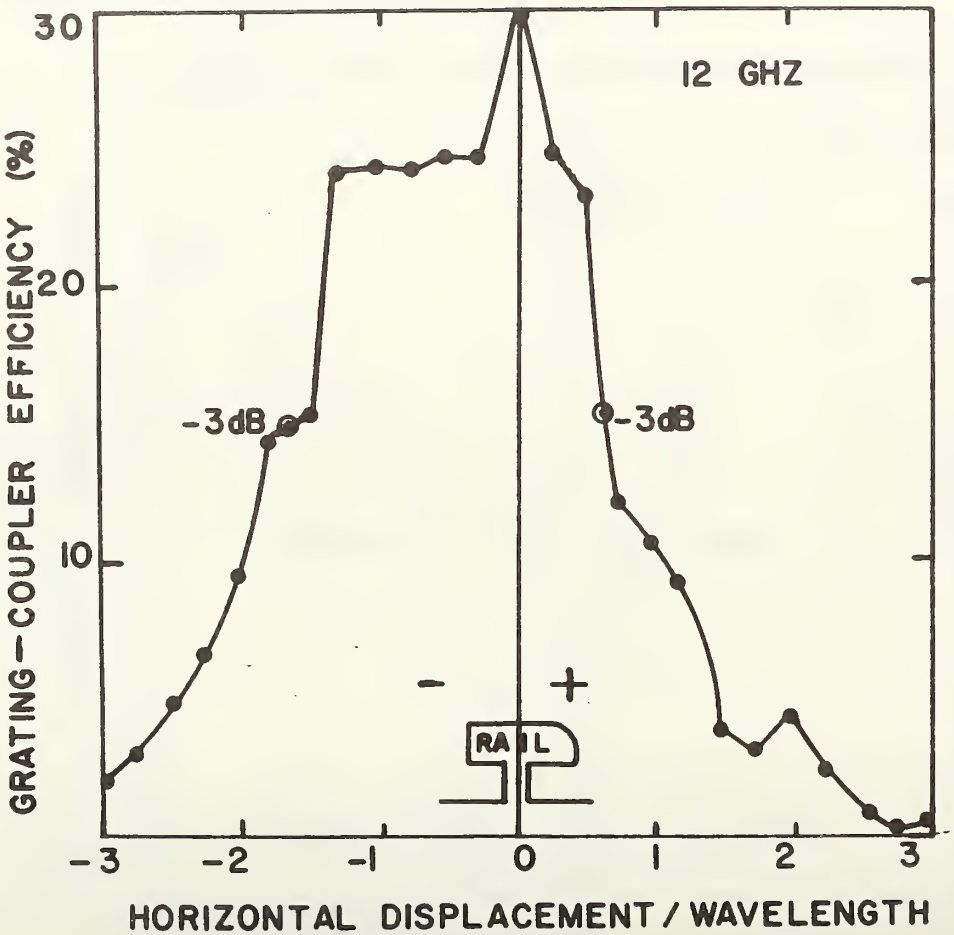


FIGURE 12. GRATING-COUPLER EXCITATION EFFICIENCY VS (HORIZONTAL DISPLACEMENT)/ (WAVELENGTH) ON STANDARD RAILROAD RAIL AT 12 GHz.

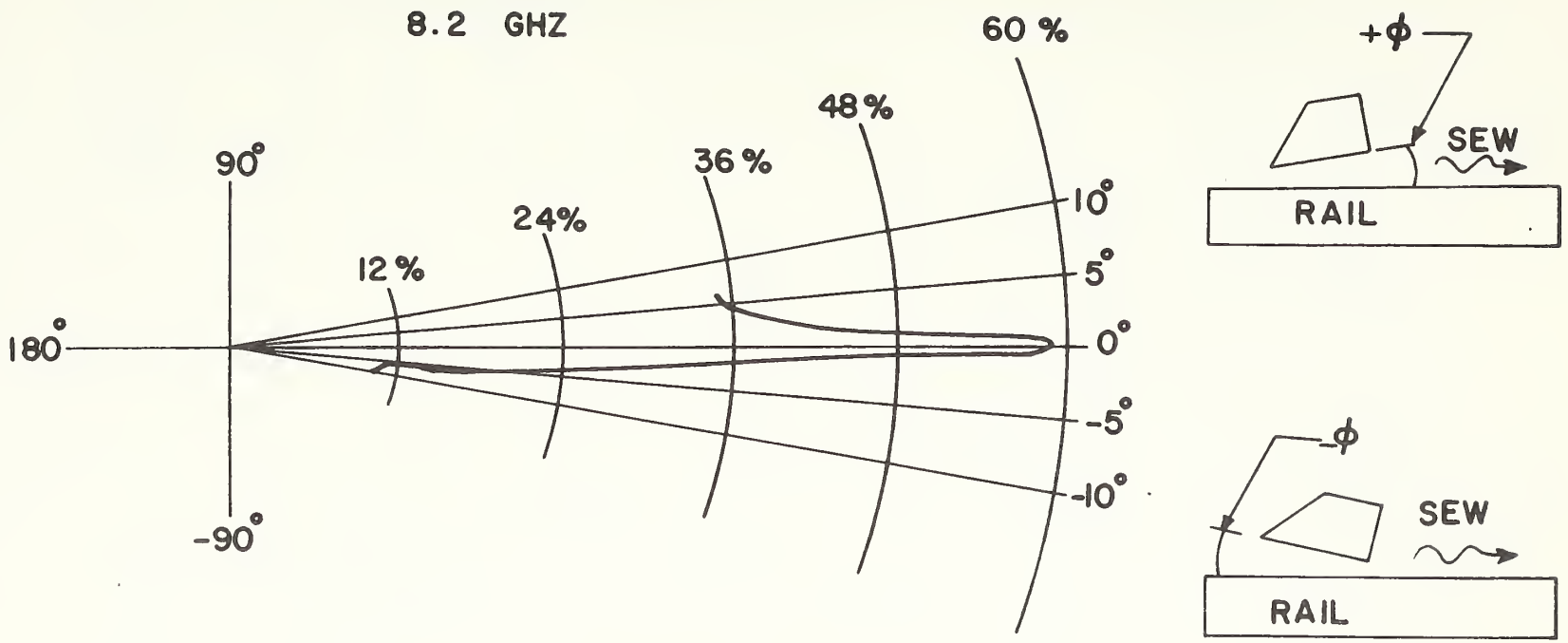


FIGURE 13. PRISM-COUPLER EXCITATION EFFICIENCY VS PITCH ANGLE ($\phi$) ON STANDARD RAILROAD RAIL AT 8.2 GHz.

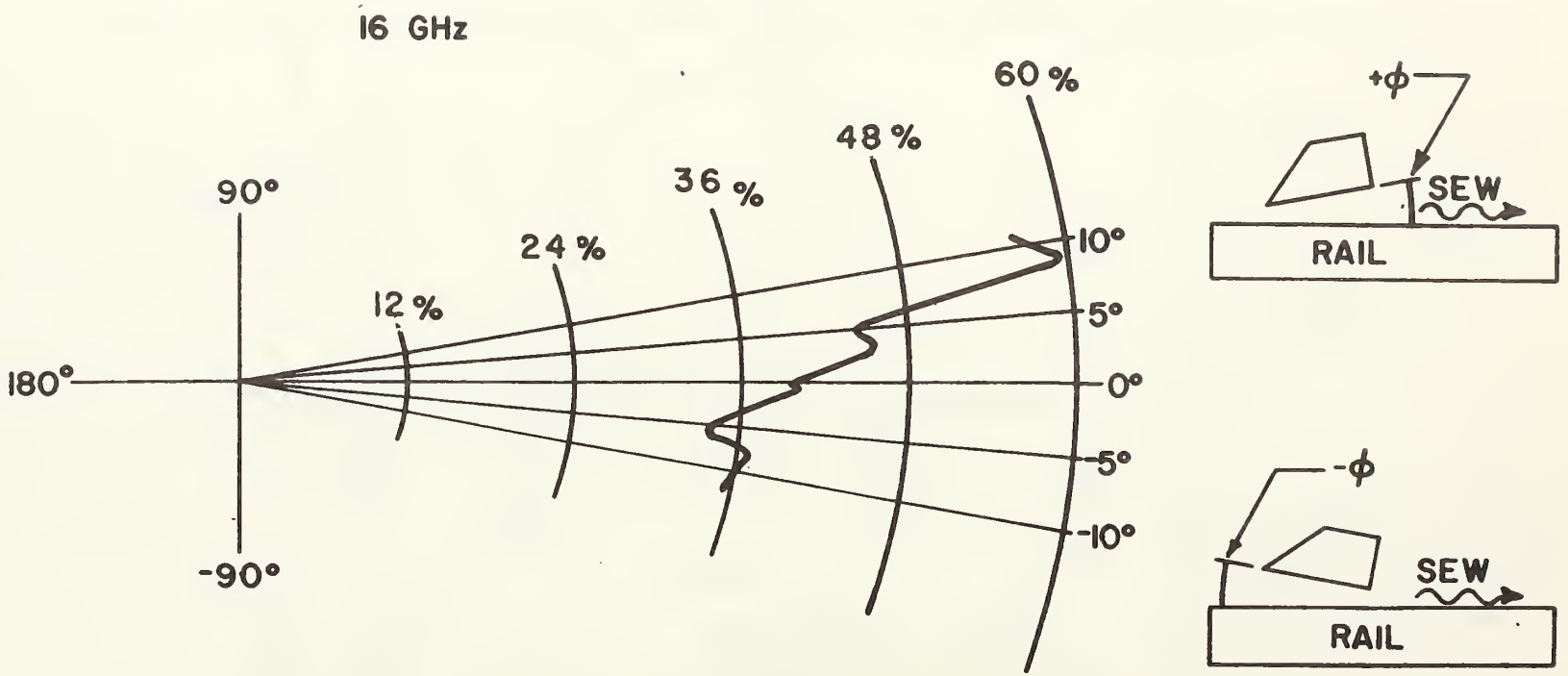


FIGURE 14. PRISM-COUPLER EXCITATION EFFICIENCY VS PITCH ANGLE (ϕ) ON STANDARD RAILROAD RAIL AT 16 GHz.

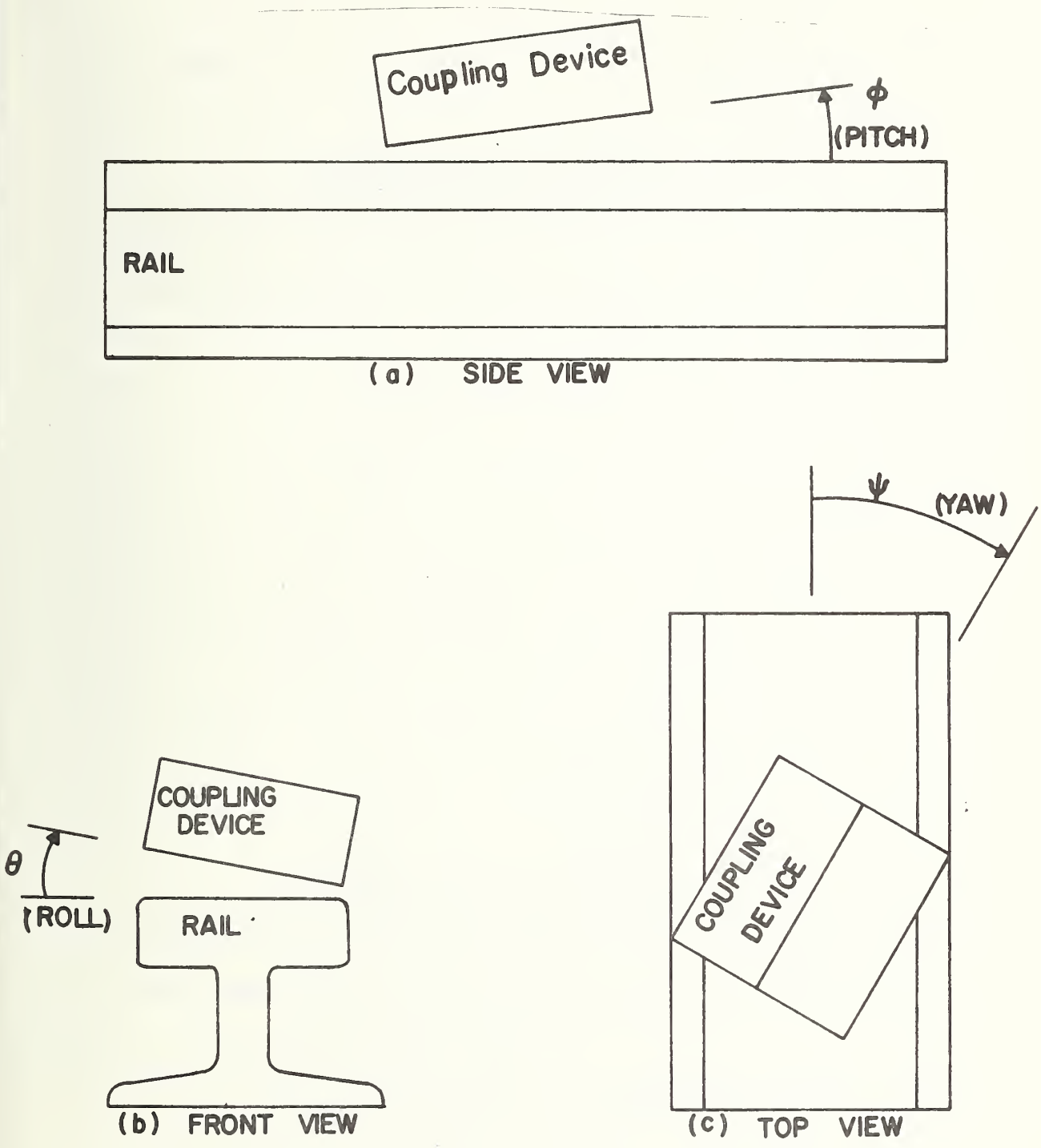


FIGURE 15. EFFECT OF (a) PITCH, (b) ROLL, (c) YAW ON SEW COUPLING EFFICIENCY.

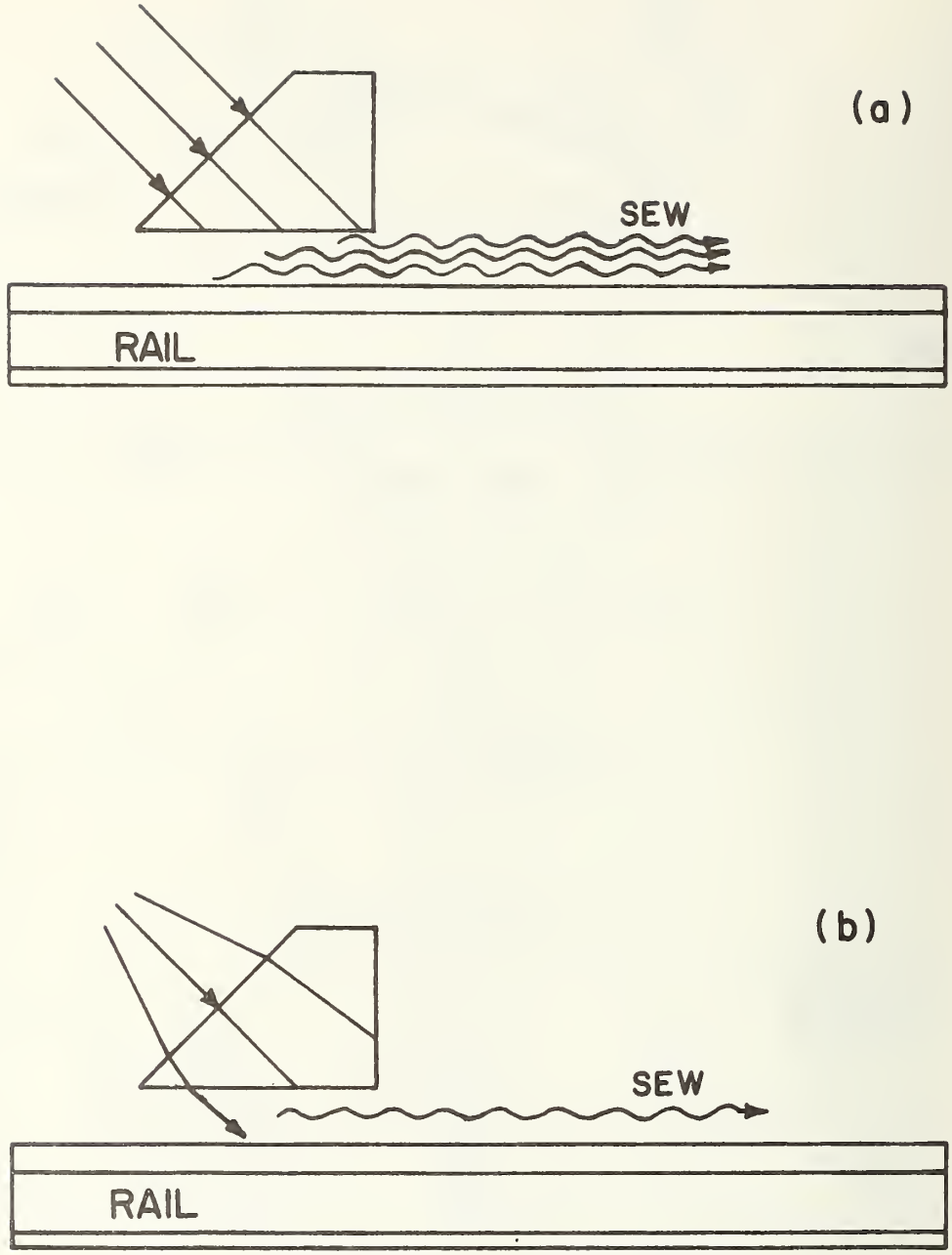


FIGURE 16. EFFECT OF (a) PARALLEL BEAM AND (b) UNPARALLEL BEAM ON PRISM-COUPLER EXCITATION EFFICIENCY.

is refracted along the base of the prism where it is normally captured along the rail-air interface of the railroad rail. If the beam is divergent, as in the case of a horn antenna taped to the back of the prism, portions of the beam are refracted at various angles which cause a lessening of the efficiency (see Fig. 16b). The portions of the beam which do not emerge parallel with the prism base now form a distributed beam which can be captured as SEW by rotating the prism. Since more power is actually available in this distributed beam, the coupling efficiency increases to a point as the prism is rotated in the positive-angle direction. When the prism is rotated in the negative-angle direction, the part of the divergent beam which will be expected to come into play has already been totally internally reflected, so that coupling efficiency decreases. This pattern can also be seen in the 16-GHz plot (Fig. 14). The maximum prism-coupling efficiencies of 57 and 60 percent are achieved with the prism near the center of the rail at 8.2 and 16 GHz, respectively.

The grating-coupling efficiencies as functions of pitch angles are shown in Fig. 17 for 2 GHz and in Fig. 18 for 4 GHz. It is pointed out that the angular scale for this part is expanded 4:1 (4 degrees show only 1 degree variation in Figs. 17 and 18), and the magnitudes are plotted in decibels reflecting power changes directly. An asymmetry in the curves exists because of the fact that the head of rail used is itself asymmetric.

The changes of coupling efficiency with respect to pitch angle will be small in a normal-size track-guided vehicle since the pitch-angle change expected in normal operation is less than 2 degrees.

### 3.4 COUPLING EFFICIENCY VS ROLL ANGLE

The prism-coupling efficiencies as functions of roll angles are shown in Figs. 19 and 20 for 8.2 and 16 GHz, respectively. The roll angle (Theta) is varied in 0.2 degree increments from 0 to ± 5 degrees and in 0.5-degree increments from ± 5 to ± 15 degrees (see Fig. 15b). An asymmetry in the curves

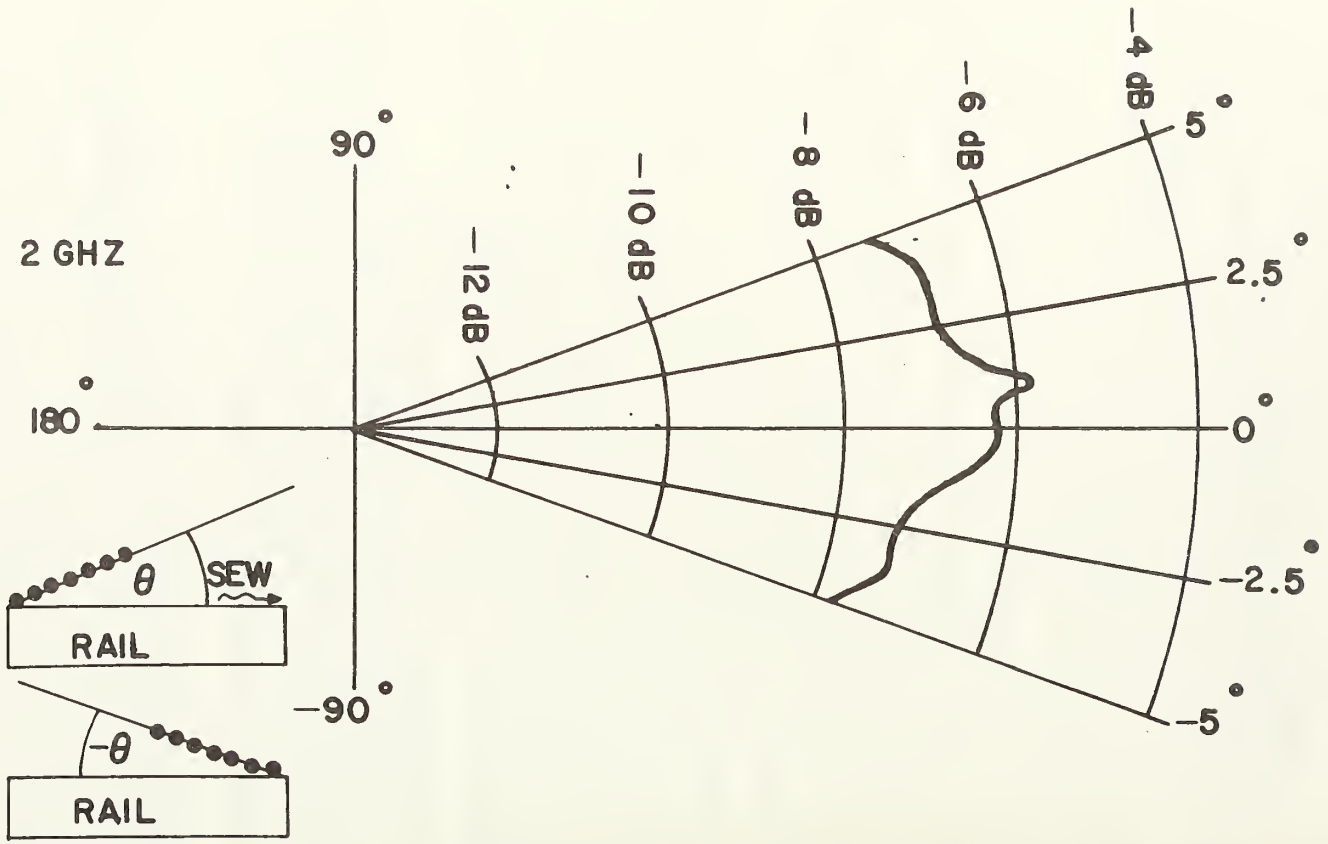


FIGURE 17. GRATING-COUPLER EXCITATION EFFICIENCY VS PITCH ANGLE ($\phi$) ON STANDARD RAILROAD RAIL AT 2 GHz.

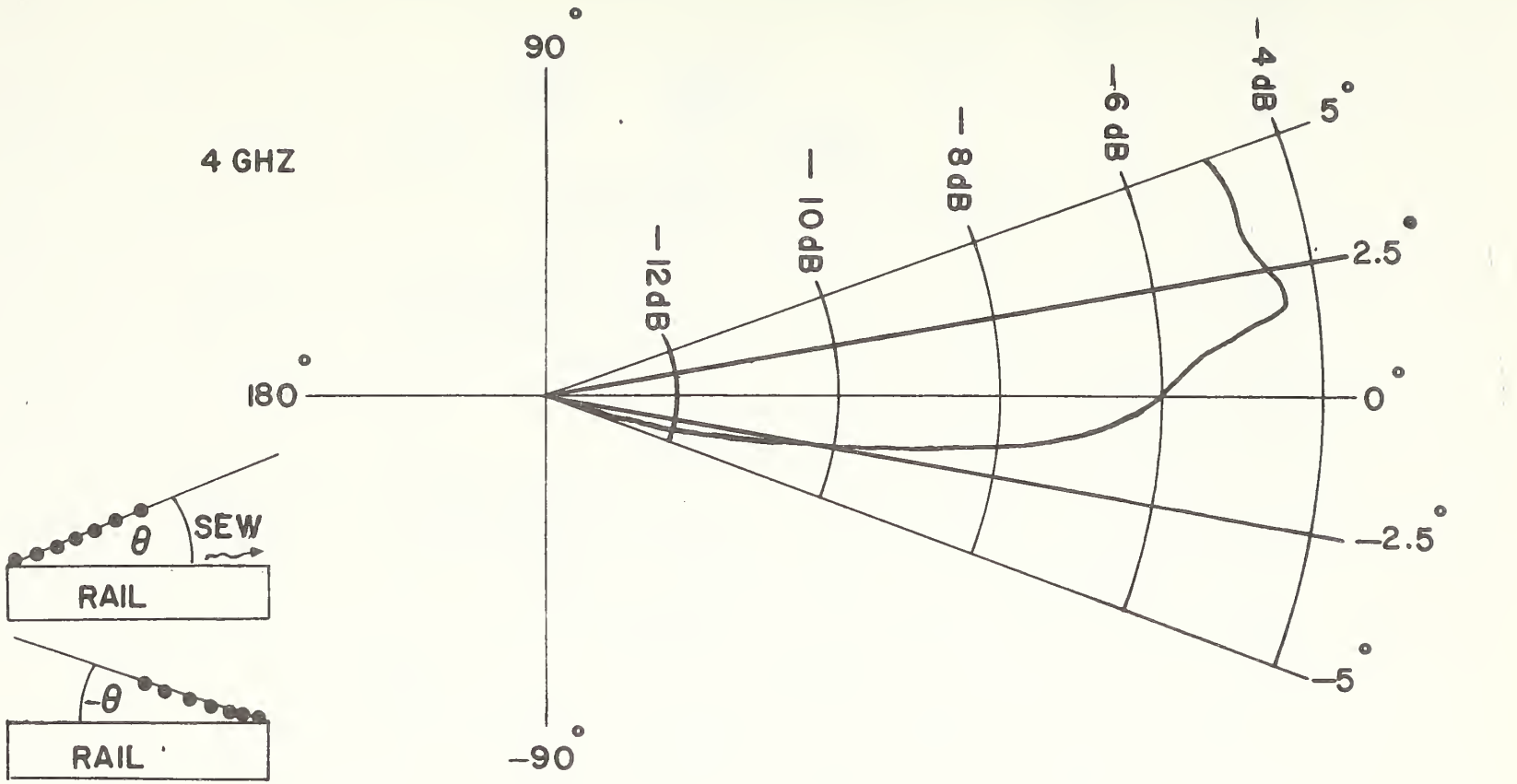


FIGURE 18. GRATING-COUPLER EXCITATION EFFICIENCY VS PITCH ANGLE ($\phi$) ON STANDARD RAILROAD RAIL AT 4 GHz.

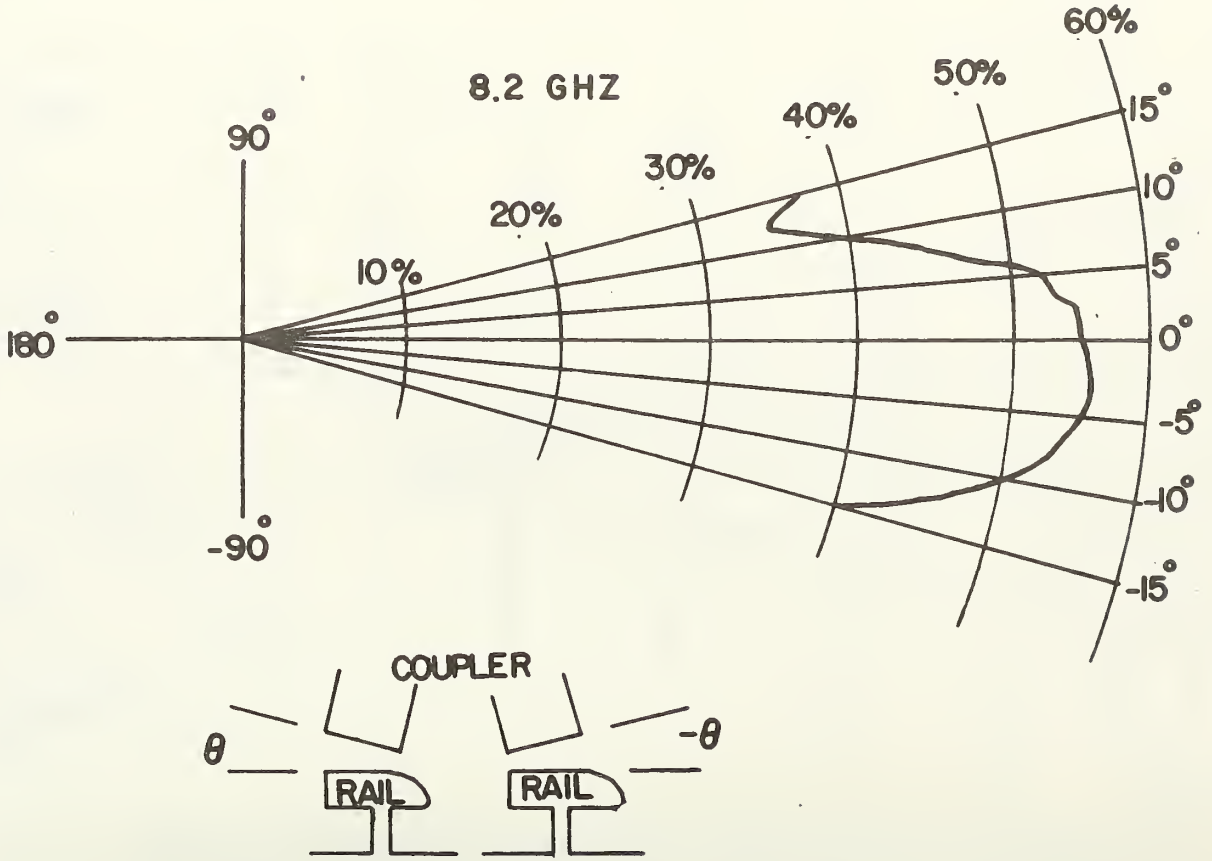


FIGURE 19. PRISM-COUPLER EXCITATION EFFICIENCY VS ROLL ANGLE (θ) ON STANDARD RAILROAD RAIL AT 8.2 GHz.

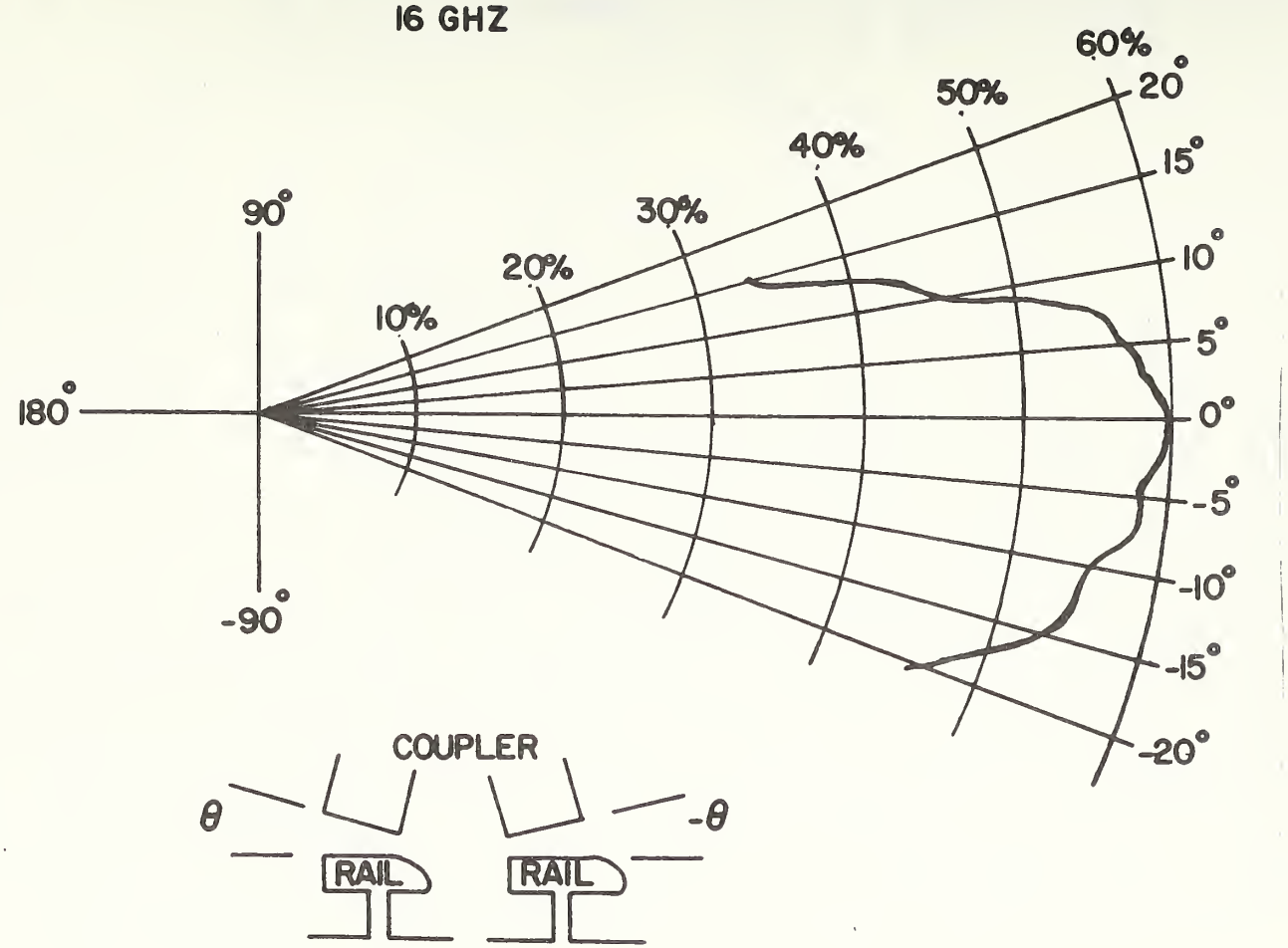


FIGURE 20. PRISM-COUPLER EXCITATION EFFICIENCY VS ROLL ANGLE (θ) ON STANDARD RAILROAD RAIL AT 16 GHz.

exists because of the fact that the head of the rail used is itself asymmetric. At 8.2 GHz when the coupler has been rolled to a positive angle, it tried to couple to a surface which sloped away from it. This has caused a pronounced dropoff of the coupling efficiency as evidenced by a 3-dB point only 11 degrees from the horizontal. When the coupler has been rolled to a negative angle over the flatter portion of the rail head, the coupling efficiency has dropped off much more slowly. This has allowed for a 3-dB point at -15.5 degrees from the horizontal. At 16 GHz, 3-dB points have moved out to +12.5 and -25 degrees. This increase of the effective coupling angle can best be explained in terms of the wavelength. As the frequency of SEW increases, its wavelength decreases in inverse proportion. The head of the rail grows larger with respect to a wavelength as the wavelength decreases, and so it takes larger perturbations from the horizontal to affect the coupling efficiency.

The grating-coupling efficiencies as function of roll angles are shown in Figs. 21 and 22 for 8 and 12 GHz, respectively. It is pointed out that the angular scale for this part has been expanded 4:1 (4 degrees show only 1 degree variation in Figs. 21 and 22), and the magnitudes are plotted in decibels to reflect power changes directly. An asymmetry in the curves exists because of the fact that the head of the rail used is itself asymmetric. The 3-dB points for 8 GHz are at +13 and -5 degrees of roll. At 12 GHz, the 3-dB points have moved out to +12 and -6 degrees of roll.

The data for the roll angles are taken at the vertical displacement of 1.5 wavelengths to provide sufficient clearance for the wide range of roll angles desired in this study. Since this displacemnet is larger than is expected to be used in a normal application, the results have been corrected to reflect optimum vertical displacement efficiencies.

The changes in efficiency with respect to the roll angle in a normal-size track-guided vehicle will be small since the roll-angle change expected in

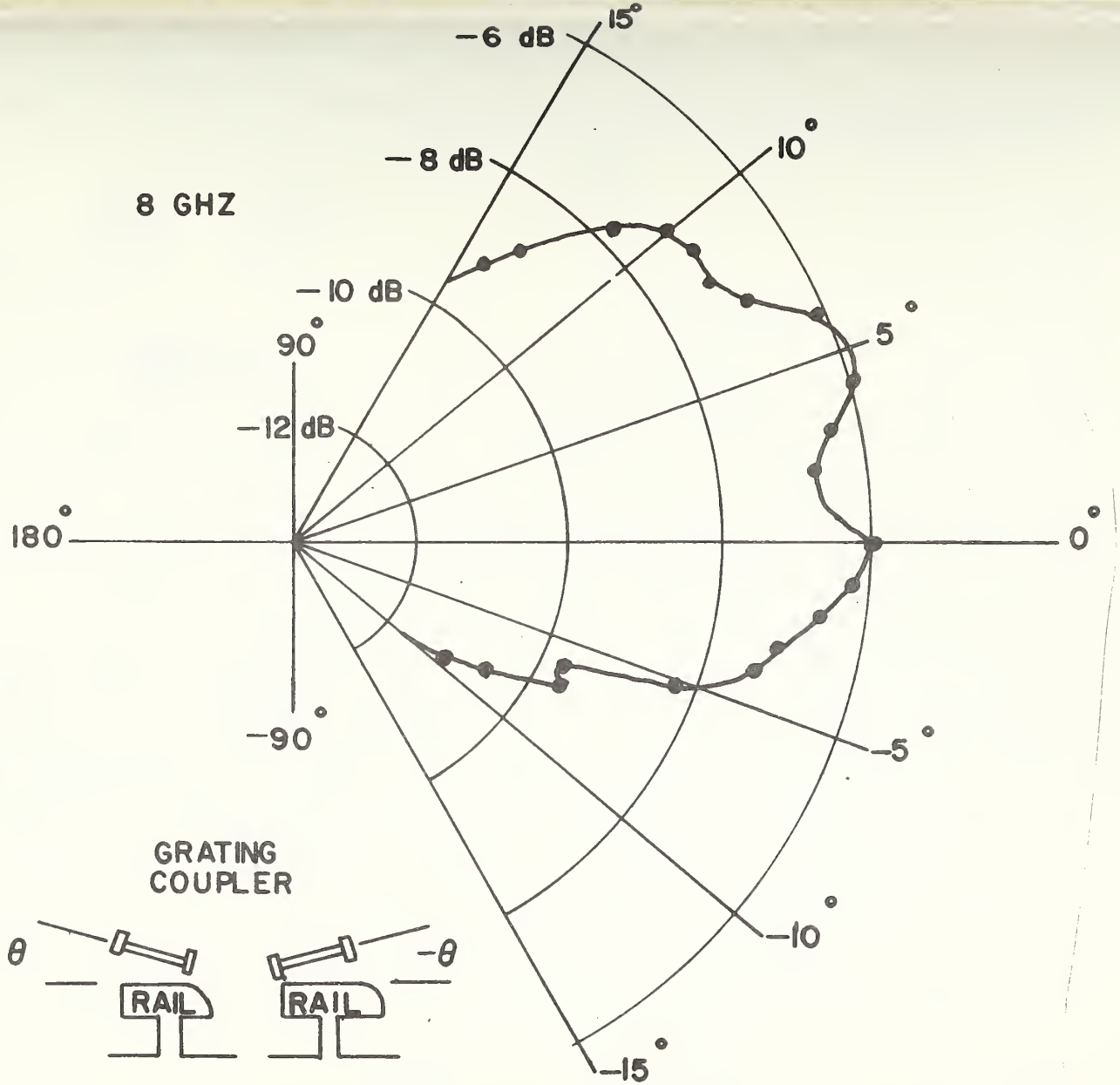


FIGURE 21. GRATING-COUPLER EXCITATION EFFICIENCY VS ROLL ANGLE (Θ) ON STANDARD RAILROAD RAIL AT 8 GHz.

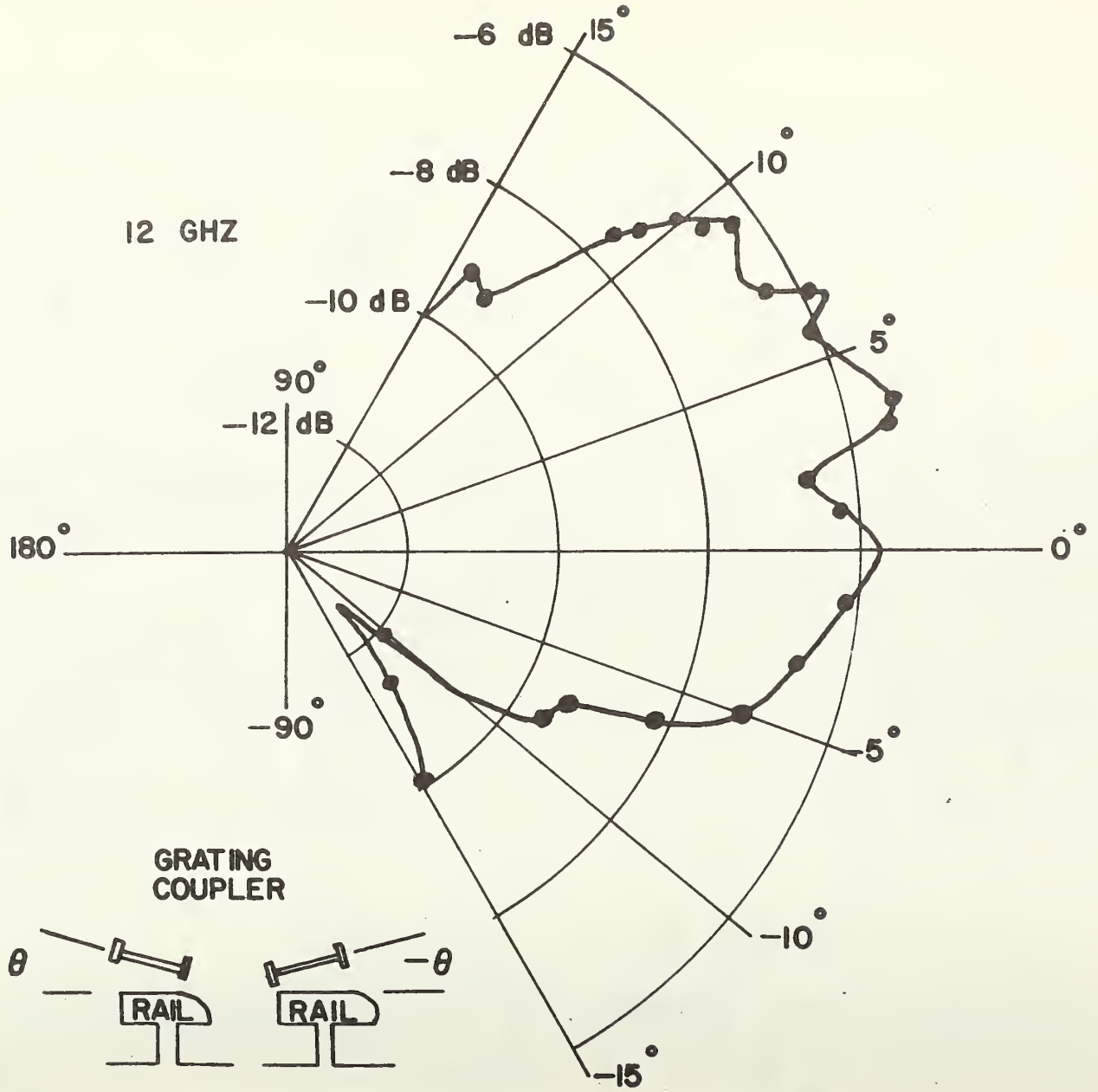


FIGURE 22. GRATING-COUPLER EXCITATION EFFICIENCY VS ROLL ANGLE (Θ) ON STANDARD RAILROAD RAIL AT 12 GHz.

normal operation will be 5 degrees or less.

## 3.5 COUPLING EFFICIENCY VS YAW ANGLE

The prism-coupling efficiencies as functions of yaw angles are shown in Figs. 23 and 24 for 8.2 and 16 GHz, respectively. The yaw angle (Psi) is varied in 0.2-degree increments from 0 to ± 15 degrees and in 0.5-degree increments from ± 5 to ± 15 degrees at the optimum vertical displacement determined in 3.1 (see Fig. 15c). The data are not symmetric because the rail is not symmetric. The 3-dB points occur at yaw angles of 12 and -15 degrees for 8 GHz and 11 and -13 degrees for 16 GHz.

The change in efficiency with respect to yaw angle for a normal-size track-guided vehicle will be small since the yaw-angle change expected in normal operation is less than 5 degrees.

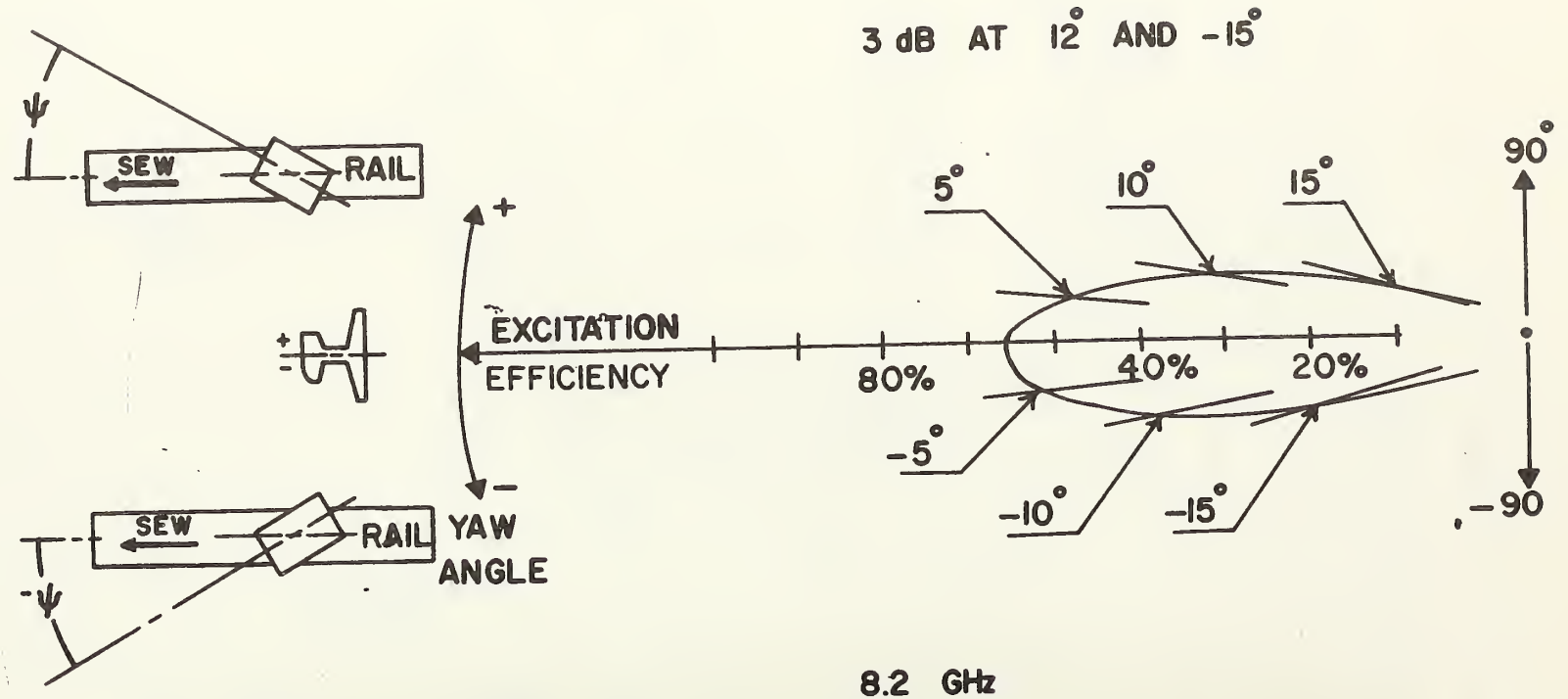


FIGURE 23. PRISM-COUPLER EXCITATION EFFICIENCY VS YAW ANGLE ($\psi$) ON STANDARD RAILROAD RAIL AT 8.2 GHz.

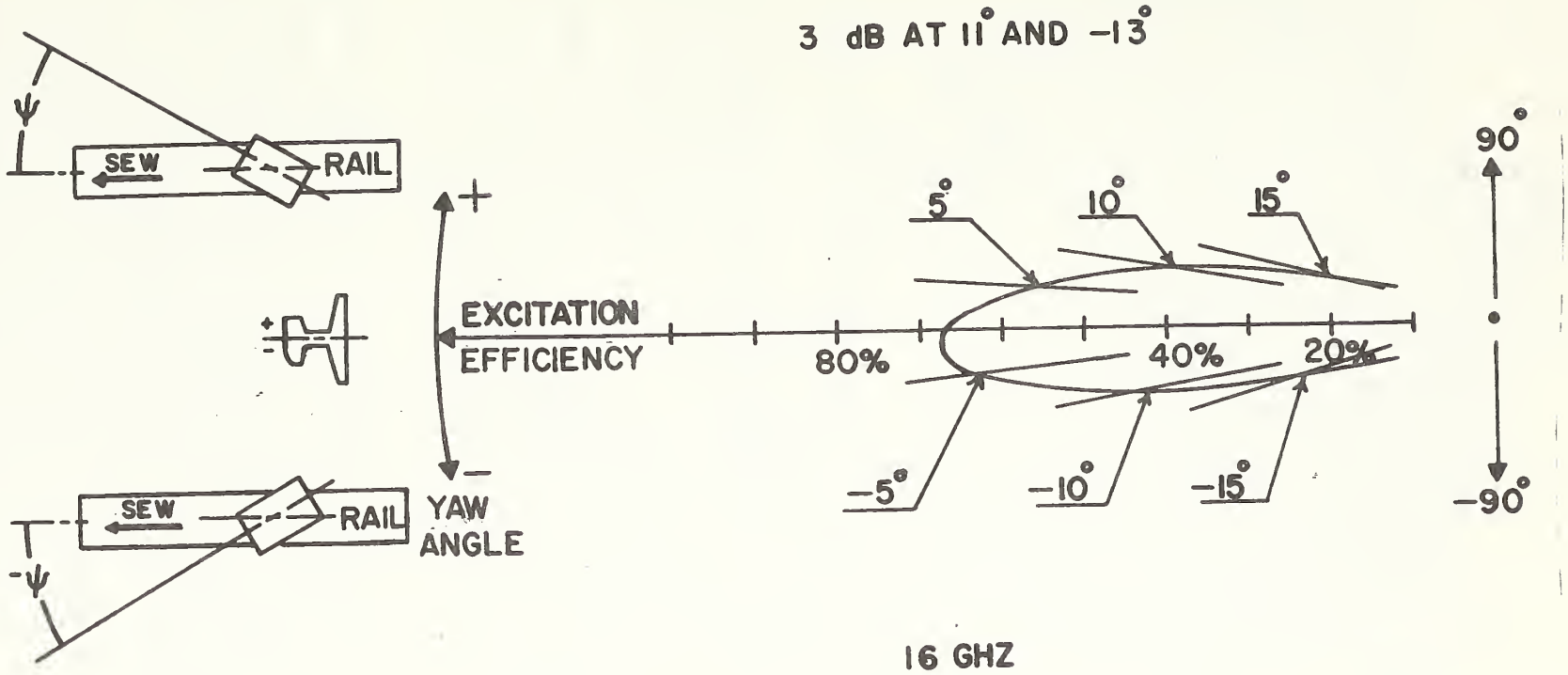


FIGURE 24. PRISM-COUPLER EXCITATION EFFICIENCY VS YAW ANGLE ($\psi$) ON STANDARD RAILROAD RAIL AT 16 GHz.

## 4. SCATTERED RADIATION PATTERNS

Measurement of scattered radiation patterns have been made on two types of SEW couplers (prism and grating) in the vicinity of the rail and in isolation. Polar-radiation patterns of each coupler in isolation are produced at several discrete microwave frequencies as a function of angle for three mutually perpendicular planes (see Fig. 25a). These are the horizontal plane (x-y plane, Angle $\phi$); the vertical plane parallel to the primary axis of the coupler (x-z plane, Angle $\psi$), and the vertical plane perpendicular to the primary axis of the coupler (y-z plane, Angle $\theta$). Data have been taken in 5-degree increments around the complete circles described in each plane, and the readings are normalized to 1 mW (dBm).

Similar measurements have been made in the vicinity of the rail, but only for the upper hemisphere (see Fig. 25b).

The experimental arrangement of the scattered radiation-pattern measurements will be discussed in 4.1. For the grating-coupler experiments, both the transmitting and receiving antennas have a reflector diameter of 45.72 cm (18 inches). The antennas are linearly polarized with 3-dB beamwidth at 6 degrees at 10 GHz. Each grating is composed of several aluminum bars with diameters of 1.27 cm. The spacing between the bars is determined from Eq. (15) for the first-order mode (m = 1).

For the prixm-coupler experiments, a horn antenna has replaced the transmitting parabolic-dish antenna. The mouth of the horn antenna has been taped to the back of the right-angle polyehylene prism. Note that the prism-coupler angle is chosen so that an electromagnetic beam normally incident on the prism face strikes the prism base at the critical angle. These prism couplers are of soft polyethylene with a relative dielectric constant of 2.25.

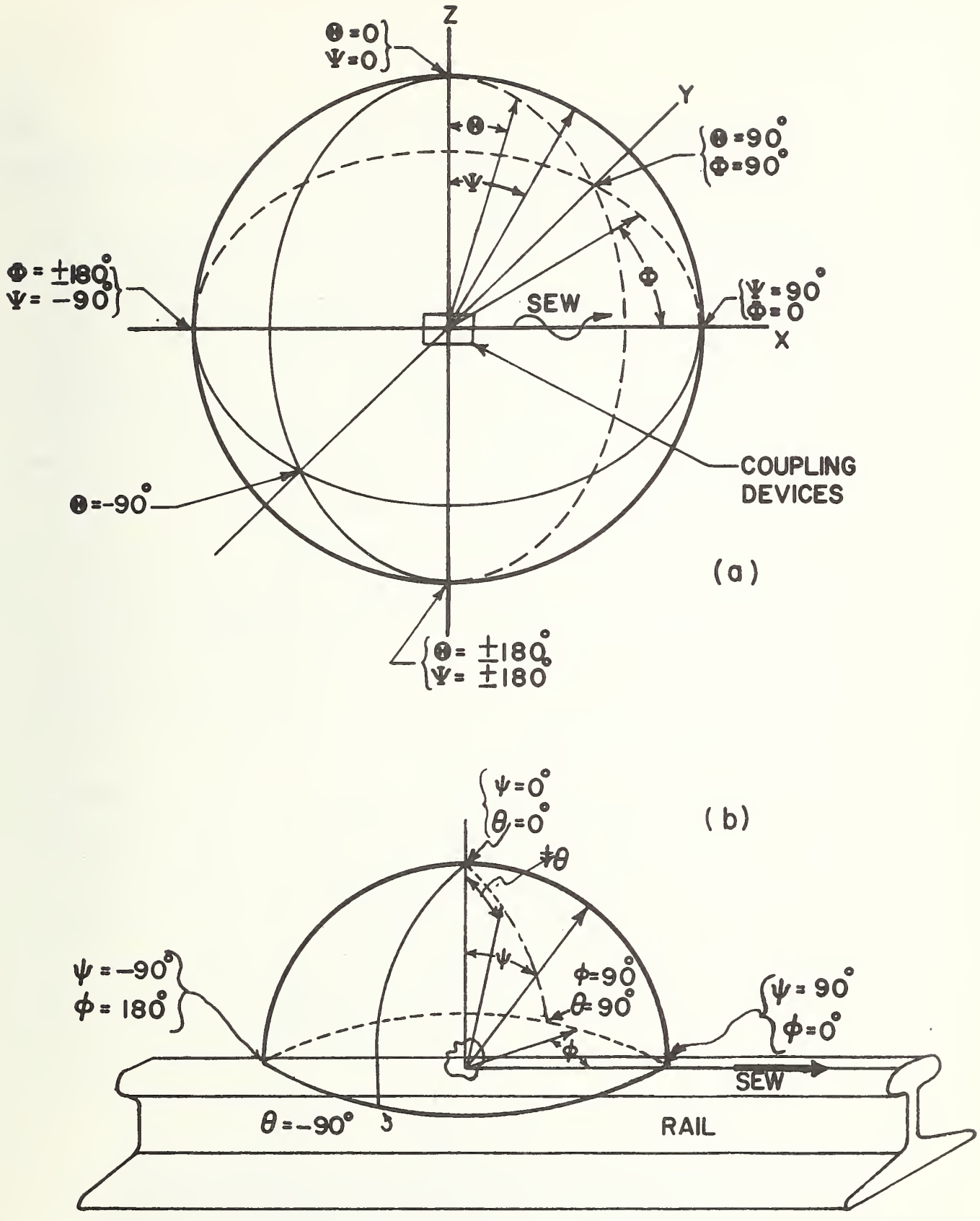


FIGURE 25. (a) HEMISPHERIC RADIATION PATTERN AND (b) UPPER HEMISPHERIC RADIATION PATTERN IN VICINITY OF RAIL.

## 4.1 SCATTERED RADIATION-PATTERN EXPERIMENTAL SETUP

To make measurements of the radiation patterns in the three mutually perpendicular planes, the following procedure is followed:

a. A support apparatus is constructed to hold the rail, transmitting antenna, and couplers. This apparatus is shown in Fig. 26.

b. The support apparatus is assembled and placed on top of an accurately marked angular measurement stand. This experiment is conducted in a very large open area. The receiving antenna is mounted on a stand 5 meters from the coupler on the support platform. The receiving antenna is sighted level to the same horizontal plane as the transmitting coupler using a transit.

c. The electronic instruments used are connected as shown in Fig. 27.

d. The sweep oscillator is adjusted to operate at a fixed frequency, appropriate for the test being performed, using the electronic frequency counter.

e. The ratiometer is calibrated following the procedure specified in its operation manuals.

f. The angle measurements are taken by rotating the angular measurement stand in 5-degree increments. Data are taken at these positions by positioning the pen of the x-y recorder to an x-axis location corresponding to the angular position, and lowering the pen to make an ink dot with a y-coordinate whose value is proportional to the ratio of the received signal to the transmitted signal. The y-axis is then calibrated in dBm (decibels down relative to 1 mW) by reading the dBm value from the ratiometer. The coupling factor of the directional coupler is added to its value and is then recorded for a given data point.

## 4.2 CALCULATION OF ELECTRIC FIELD INTENSITY AT 100 FEET (30.48 METERS)

The distance between the transmitting coupler (prism or grating) and

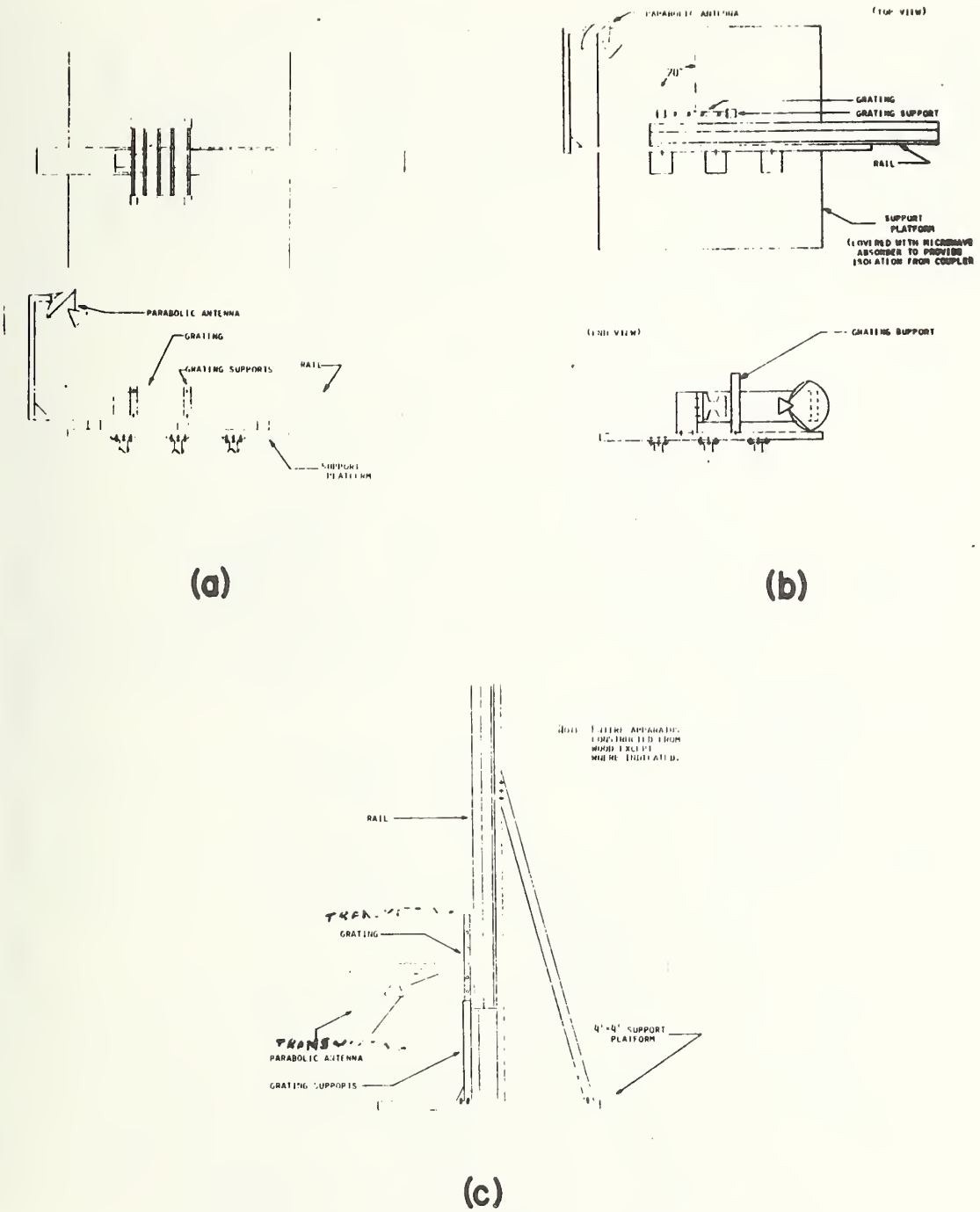


FIGURE 26. SUPPORT APPARATUS TO HOLD RAIL-TRANSMITTED ANTENNA AND COUPLER FOR MEASURING SCATTERED RADIATION PATTERN OF GRATING-RAIL COMBINATION IN (a) HORIZONTAL PLANE, (b) VERTICAL PLANE PARALLEL TO THE PRIMARY AXIS OF COUPLER, AND (c) VERTICAL PLANE PERPENDICULAR TO PRIMARY AXIS OF COUPLER.

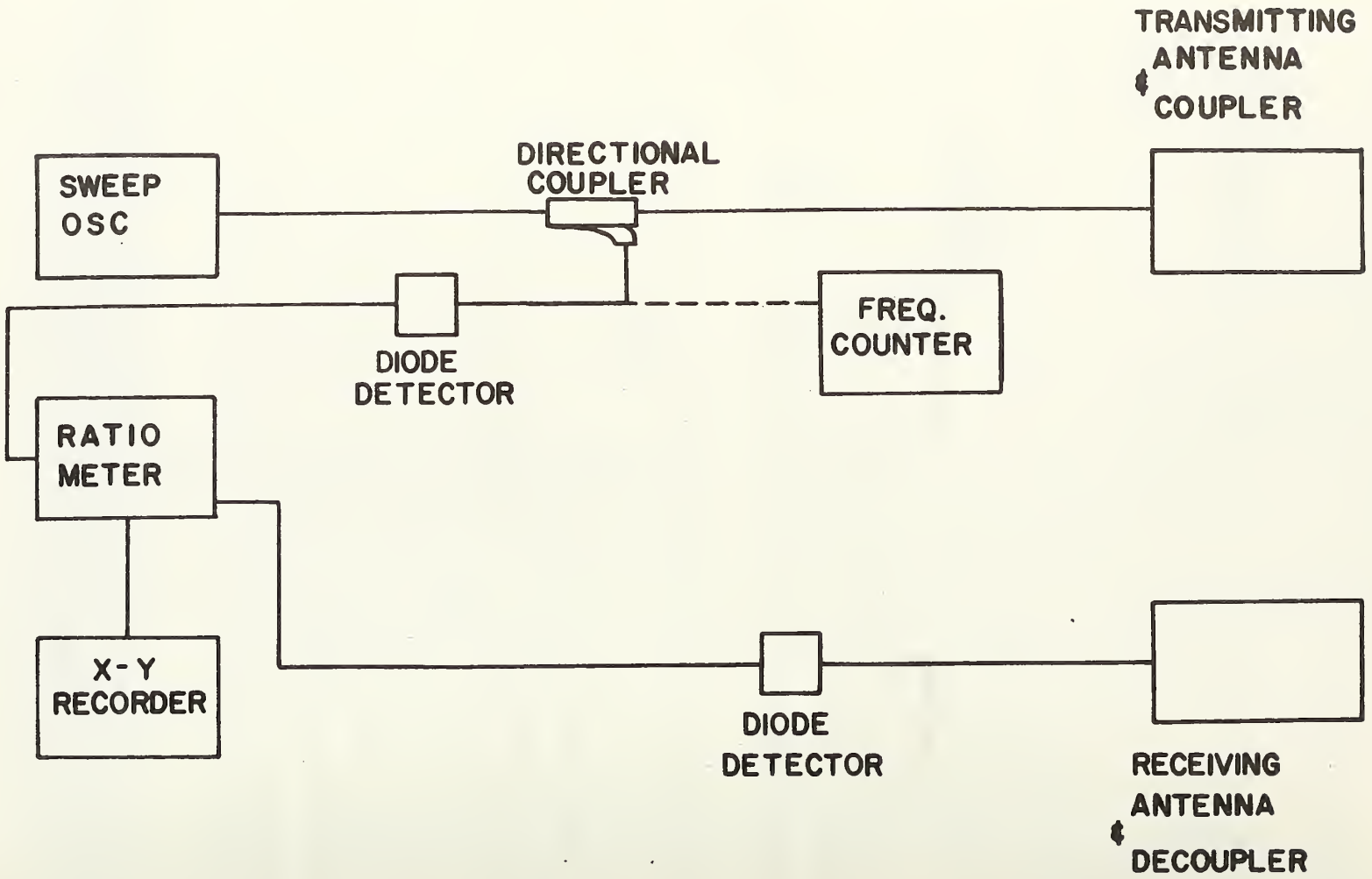


FIGURE 27. EXPERIMENTAL SETUP FOR SCATTERED RADIATION-PATTERN MEASUREMENTS.

receiving antenna has been fixed to 5 meters for all cases. The transmitting and receiving antennas are identical with a reflector diameter of 45.72 cm (18 inches). The antennas are linearly polarized with 3-dB beamwidth of 6 degrees at 10 GHz.

The power radiated per unit area in any direction is given by the Poynting vector, $\vec{P}$. For the distant or radiation field for which electric field intensity $\vec{E}$ and magnetic field intensity $\vec{H}$ are orthogonal in a plane normal to the radius vector, and for which $E = \eta_v H$ where $\eta_v$ is the intrinsic impedance of free space, the power flow per unit area is given by

$$P = \frac{E^2}{\eta_v} = \frac{E^2}{120\pi} \quad W/m^2 \quad . \tag{16}$$

Power densities at points $P_o$ (5 m from coupler) and $P_1$ (30.48 m from coupler) are as follows (see Fig. 28):

$$\text{At } P_o, \qquad P_o = \frac{W_c G_c}{4\pi R_o^2} = \frac{W_R}{A_R} \quad . \tag{17}$$

$$\text{At } P_1, \qquad P_1 = \frac{W_c G_c}{4\pi R_1^2} \quad . \tag{18}$$

Where $W_c$ is the radiated power at the coupler, $G_c$ is gain in the arrow direction (see Fig. 28), $R_o$ is the distance between coupler and receiver (5 m), $W_R$ is the received power at 5 m, $A_R$ is the effective area of receiving antenna, and $R_1$ is 30.48 m. From Eq. (17), we get

$$W_c G_c = 4\pi R_o^2 \frac{W_R}{A_R} \quad . \tag{19}$$

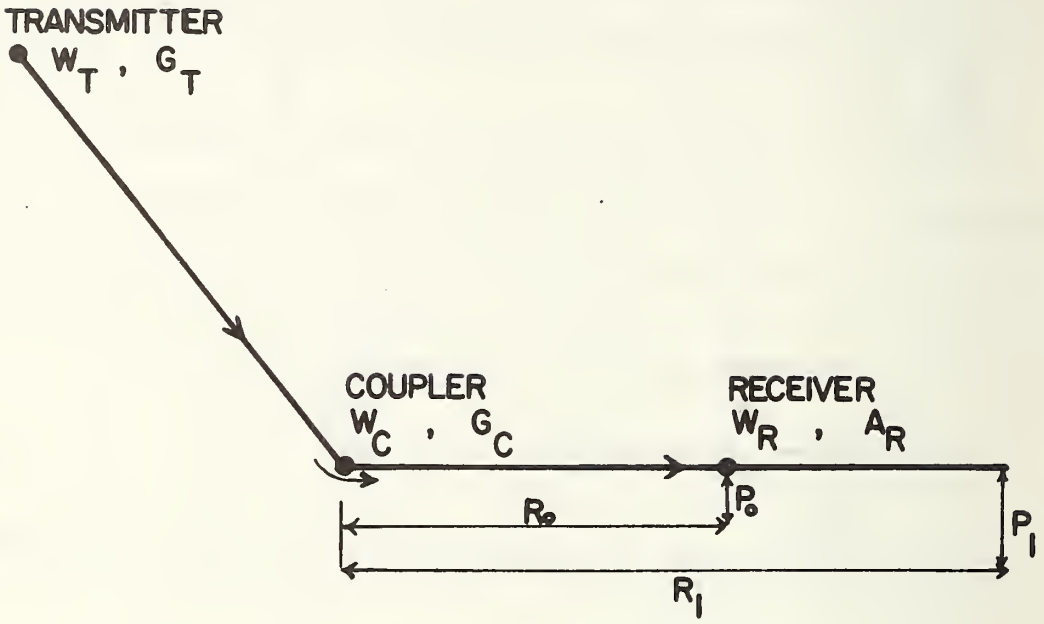


FIGURE 28. LOCATIONS OF TRANSMITTER, COUPLER, AND RECEIVER FOR SCATTERED RADIATION-PATTERN MEASUREMENTS.

Substituting Eq. (19) in Eq. (18) results in

$$P_1 = \left(\frac{R_o}{R_1}\right)^2 \frac{W_R}{A_R} \quad . \tag{20}$$

The power density at point $P_1$ from Eq. (16) is

$$P_1 = \frac{E_1^2}{120\pi} \quad . \tag{21}$$

Equating Eqs. (20) and (21), we get

$$E_1^2 = 120\pi \frac{W_R}{A_R} \left(\frac{R_o}{R_1}\right)^2 \quad . \tag{22}$$

The area of the antenna reflector is given by

$$A_R = \frac{\pi D^2}{4} \quad . \tag{23}$$

Since the diameter of the antenna is 45.72 cm, we obtain from Eq. (23)

$$A_R = 0.16417 \text{ m}^2 \quad . \tag{24}$$

Substituting Eq. (24) and all the known values in Eq. (22) result in

$$E_1^2 = 120\pi \frac{W_R}{0.16417} \left(\frac{5}{30.48}\right)^2 = 61.79 \, W_R \quad . \tag{25}$$

The electric field intensity at 100 feet (30.48 m) is

$$E_1 = 7.86 \sqrt{W_R} \quad \text{(V/m)}, \tag{26}$$

where $W_R$ is the received power (watts)at 5 m.

## 4.3 SCATTERED RADIATION PATTERN IN HORIZONTAL PLANE

The maximum received signals relative to 1 mW (dBm) and the corresponding electric field intensity (E) at several frequencies for different configurations are as follows:

a) Grating-- No Rail (Fig. 29)

| Frequency (GHz) | 2 | 4 | 8 |
|---|---|---|---|
| Maximum received power at 5 m (dBm) | -23 | -29 | -40 |
| Maximum E at 100' (mV/m) | 17.596 | 8.819 | 2.486. |

b) Grating-- Rail (Fig. 30)

| Frequency (GHz) | 2 | 4 | 8 |
|---|---|---|---|
| Maximum received power at 5 m (dBm) | -22 | -31 | -33 |
| Maximum E at 100' (mV/m) | 19.743 | 7.005 | 5.564. |

c) Prism-- No Rail (Fig. 31)

| Frequency (GHz) | 8 | 12 | 16.2 |
|---|---|---|---|
| Maximum received power at 5 m (dBm) | -23 | -30 | -44 |
| Maximum E at 100' (mV/m) | 17.596 | 7.860 | 1.568. |

d) Prism-- Rail (Fig. 32)

| Frequency (GHz) | 8 | 12 | 16.2 |
|---|---|---|---|
| Maximum received power at 5 m (dBm) | -24 | -35 | -43 |
| Maximum E at 100' (mV/m) | 15.683 | 4.420 | 1.760. |

The results of radiation-pattern data in the horizontal plane for both the grating-and-prism couplers show that to meet the FCC specification of 500 μV/m at 100 ft, the couplers must be redesigned. Redesigning the couplers will involve the use of absorbing materials around the couplers to reduce the radiating power in the nontransmitting directions which exceed FCC limits

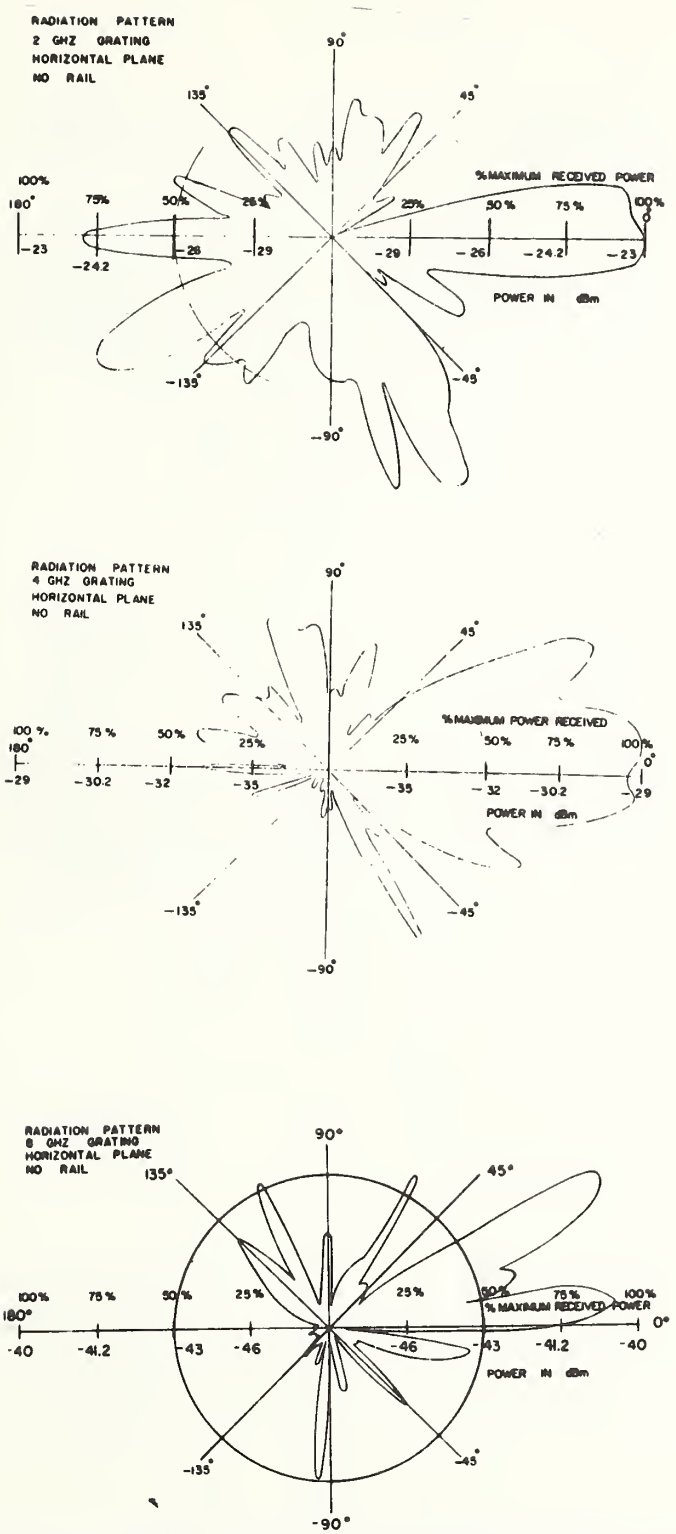


FIGURE 29. RADIATION PATTERNS GRATING IN HORIZONTAL PLANE IN ISOLATION FROM RAIL AT 2, 4, and 8 GHz.

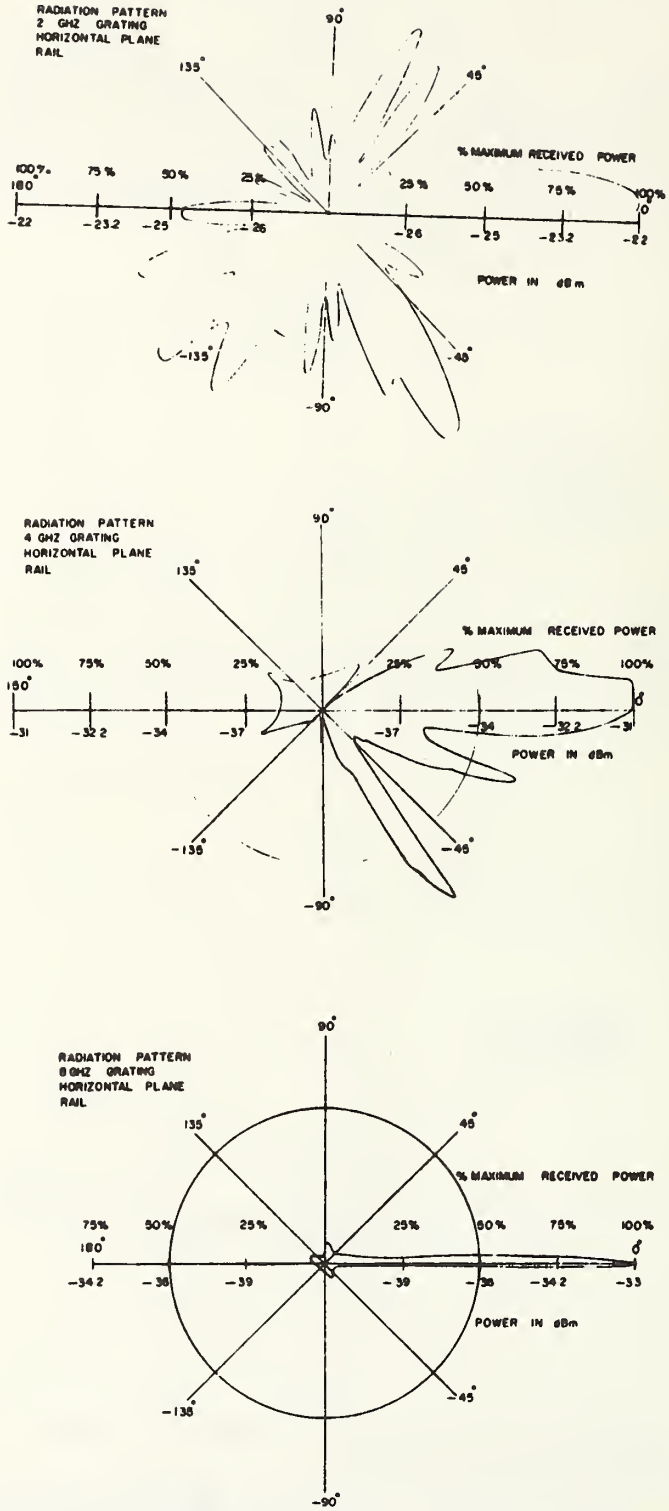


FIGURE 30. RADIATION PATTERNS OF GRATING IN HORIZONTAL PLANE IN VICINITY OF RAIL AT 2, 4, and 8 GHZ.

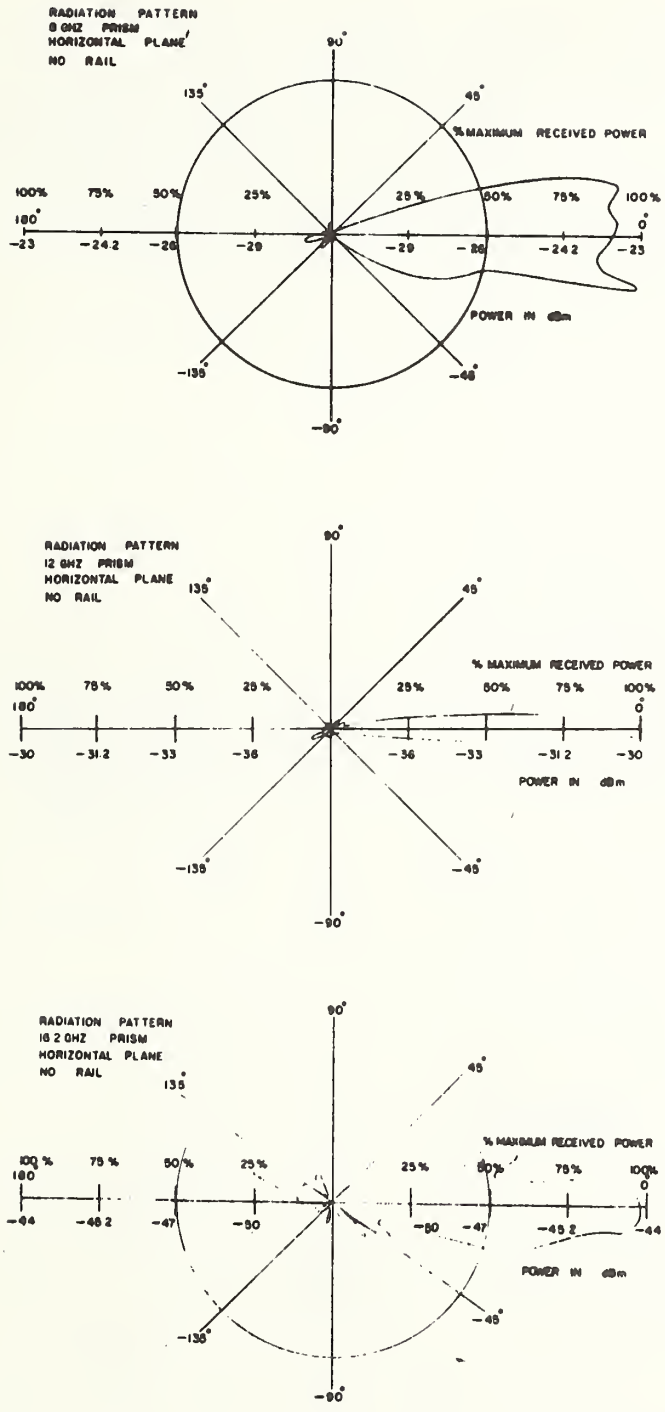


FIGURE 31. RADIATION PATTERNS OF PRISM IN HORIZONTAL PLANE IN ISOLATION FROM RAIL AT 8, 12, and 16.2 GHz.

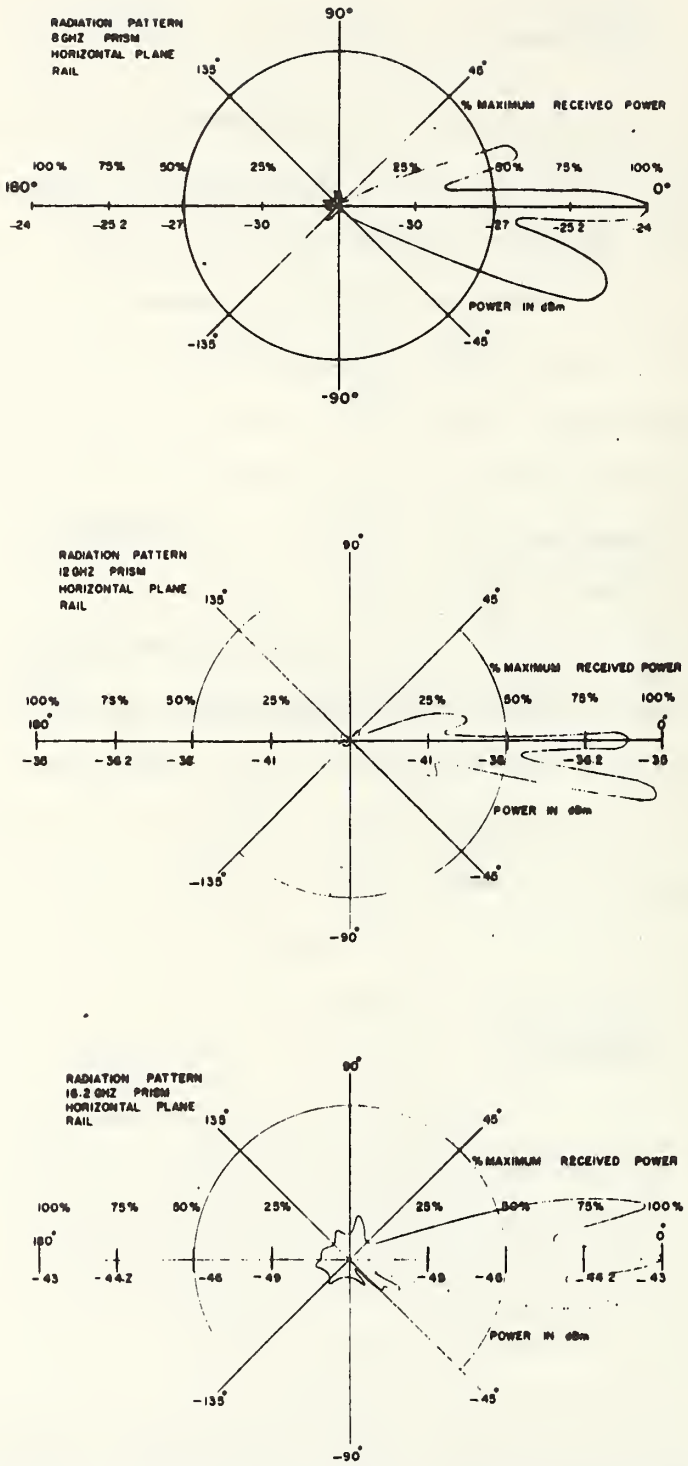


FIGURE 32. RADIATION PATTERNS OF PRISM IN HORIZONTAL PLANE IN VICINITY OF RAIL AT 8, 12, and 16.2 GHz.

## 4.4 SCATTERED RADIATION PATTERNS IN VERTICAL PLANE PARALLEL TO PRIMARY AXIS OF COUPLER AND VERTICAL PLANE PERPENDICULAR TO PRIMARY AXIS OF COUPLER

For the grating coupler, the positions of the maximum signals in the vertical plane parallel to the primary axis can be predicted by

$$d(\sin \alpha + \sin \theta) = m\lambda \qquad m = 0, \pm 1, \pm 2, \ldots , \tag{27}$$

where

$d$ = grating constant ,

$m$ = order mode ,

$\theta$ = position of the maximum signal , and

$\alpha$ = incident angle of electromagnetic wave .

Since in our experiments $\frac{\lambda}{d} = 0.66$ and $\alpha = -20$ degrees, the calculated positive maximum signals are at:

$$\theta = 20^{\circ}; \ 90^{\circ}. \tag{28}$$

Experimental data are in good agreement with these calculations.

Similar data to that presented in section 4.3 for the horizontal plane (x-y plane) are also available for the vertical plane parallel to the primary axis of the coupler (x-z plane) and the vertical plane perpendicular to the primary axis of the coupler (y-z plane). In these cases however, the receiving antenna is not always oriented with the same polarization as the transmitting antenna, and the data need to be corrected by adding or subtracting a constant to all readings. Even without this correction, it is clear that the couplers need to be redesigned to meet the FCC specification for operation without a license.

## 5. DISCUSSION AND CONCLUSIONS

The SEW excitation efficiencies for both the prism and grating coupling techniques in the vicinity of the railroad rail have been measured. The coupling experiments have included studies of the SEW excitation efficiencies as functions of the frequency, vertical displacement of the coupler above the rail, horizontal (lateral) displacement of the coupler from rail center, pitch angle of the coupler, roll angle of the coupler, and yaw angle of the coupler.

The SEW coupling efficiency curves for both prism-and-grating couplers show dependence on vertical displacement above the rail, on horizontal displacement of the coupler from rail center; and on pitch, roll, and yaw angles of the coupler relative to the rail.

The maximum peak for the prism coupler occurs at one-half-wavelength gap spacing in vertical displacement between the prism coupler and the rail head for the frequencies considered. For the grating coupler, the peaks are repeated every half-wavelength, and the index of the maximum peak appears to increase with increasing frequency.

The maximum excitation efficiency of the prism-coupling technique is about 60 percent at 16 GHz vs about 30 percent for the grating coupling technique at 12 GHz. Reducing the frequency causes an efficiency reduction for the prism (57 percent at 8 GHz) and for the grating (26 percent at 8 GHz). For both couplers, the efficiencies vs horizontal displacement; pitch, roll, and yaw angles fall off asymmetrically. The asymmetry in the data is attributed to the rail's asymmetry. This effect is relatively more pronounced when the wavelength is smaller, as expected, since the ratio of the wavelength to the rail dimension is smaller.

The falloff in coupling efficiency with horizontal displacement is very small until half the coupler is displaced from over the rail head. The 3-dB points are at, or greater than, one-half the coupler-width displacement (10.16/2 = 5.08 cm), whereas one does not expect even one-quarter the coupler-width displacement. For pitch-angular deviation, there is only a small fall-off in coupling efficiency to the 2-degree expected pitch-angular deviation and is usable to and beyond (for positive pitch-angular deviation) 5 degrees. The falloff in efficiency for roll-and-yaw angular deviation is small to the maximum 5 degrees expected in normal use, and usable to more than 15-degree roll-and-yaw angular deviation.

Polar-radiation patterns of each coupler in isolation are produced at several discrete microwave frequencies as functions of angles for three mutually perpendicular planes. These are horizontal plane (x-y plane, Angle $\phi$), vertical plane parallel to the primary axis of the coupler (x-z plane, Angle $\psi$), and vertical plane perpendicular to the primary axis of the coupler (x-z plane, Angle $\theta$). Similar measurements are made in the vicinity of the rail but only for the upper hemisphere.

The results of radiation-pattern data show that to meet the FCC fication of 500 μV/m at 100 ft for no license, the couplers must be redesigned. Redesigning the couplers involve the use of microwave energy-absorbing material around the couplers to reduce the readiating power in nontransmitting directions which exceeds FCC limits.

Appropriate absorbing materials are on order. and the redesigned couplers will be used in the balance of the experiments specified in the first year of this project as soon as they are available.

The data on vertical and horizontal displacements, and on roll, pitch, and and yaw angles indicate that either the prism or grating couplers mounted on a

moving vehicle will operate successfully for the linear displacements and the angular deviation that one will normally expect to encounter on a track-guided vehicle.

## REFERENCES


1. S. F. Mahmoud and J. C. Beal, "Obstruction Detection Program: Final Report", RCA David Sarnoff Res. Cent., Submitted to U.S. Dept. of Transportation, 1969.

2. R. E. Fenton, R. L. Cosgriff, K. W. Olson and L. M. Blackwell, "A Surface Wave Transmission Line for Vehicular Communications", Final Tech. Rep. for U.S. Dept. of Transportation Office of High Speed Ground Transportation by U.S. Dept. of Commerce/Environmental Science Administration, Boulder, Colo., Feb. 1970.

3. D. E. Magnus et al., "Obstacle Detection for High Speed Ground Transportation", U.S. Dept. of Commerce, C.F.S.T.I. PB-194-374. Rep. GENAPPSL-TR-745, June 1970.

4. A. D. McAulay, "Detection of Track-Guided Ground Vehicles Using the Track as an Electromagnetic Surface Waveguide". Report Number UMTA-PA-11-0007-73-4, Dec. 1973.

5. H. H. Ogilby, "Radar on the Railways", Electronics and Power (J. IEE), Vol. 10, pp. 146-150, May 1964.

6. F. T. Barwell and H. H. Ogilby, "Communications and Their Effect on Railway Operations", Proc. Inst. Railway Signal Eng., p.135, January 1966.

7. H. M. Barlow, "High Frequency Guided Electromagnetic Waves in Application to Railway Signalling and Control", Radio Electron. Eng., Vol. 33, pp. 275-281, May 1967.

8. Y. Amemiya, N. Kurita, T. Nakahara, N. Kurauchi and T. Nagao, "Surface Waveguides for Railway Application", Intern. Conf. Microwaves, Circuit Theory, Inform. Theory, Tokyo, 1964, Pt. I, p. 15, M1-8, Inst. Elect. Com. Japan, 1964.

9. Y. Amemiya, N. Kurita, T. Nakahara, N. Kurauchi and T. Nagao, "Surface Wave Radar System", Sumitomo Elec. Tech. Rev., Vol. 3, pp. 49-56, 1964.

10. T. Kawakami, T. Maruhama, T. Takeya and S. Kohno, "Waveguide Communication System for Centralized Railway Traffic Control", IEEE Trans. Vehicular Commun., Vol. 13, pp. 1-17, 1964.

11. Y. Amemiya, N. Kurita, K. Uematsu, T. Kakahara, N. Kurauchi and H. Kitani, "Leaky Waveguide Radar System-An Approach to Obstacle Detection for Railroads", Sumitomo Elec. Tech. Rev., Vol. 9, pp. 82-92, 1967.

12. T. Nakahara and N. Kurauchi, "Millimeter Waveguides with Applications to Railroad Communications", in Advance in Microwaves, Vol. 4, pp. 191-300, New York: Academic Press, 1969.

13. S. F. Mahmoud and J. C. Beal, "Reflection of Surface Wave on a Dielectric Image Line with Application to 'Guided' Radar", Proc. IEEE G-MTT Int. Microwave Symp. (Chicago, Ill.) pp. 139-141, May 22-24, 1972.

14. L. M. Smith, "Guided Radar Obstacle Detection for Ground Transportation Systems", M.S. Thesis, Queen's University, Kingston, Ont. Canada, 1973.

15. S. F. Mahmoud, "Electromagnetic Aspects of Guided Radar for Guided Ground Transportation", Ph.D. Dissertation, Queen's University, Kingston, Ont. Canada, 1973.

16. J. C. Beal, J. Josiak, S. F. Mahmoud and V. Rawat, "Continuous-Access Guided Communication (CAGC) for Ground-Transportation Systems", Proc. IEEE, Vol. 61, pp. 562-568, May 1973.

17. S. F. Mahmoud, "Characteristics of Electromagnetic Guided Wave for Communication in Coal Mine Tunnels," IEEE Trans. Communications, Vol. COM-22, pp. 1547-1554, October, 1974.

18. S. F. Mahmoud and J. C. Beal, "Scattering of Surface Waves by Metallic Obstacles on the Dielectric Image Line", IEEE Trans. Microwave and Techniques, Vol. MTT-23, pp. 185-192, February 1975.

19. S. F. Mahmoud and J. C. Beal, "Scattering of Surface Waves at a Dielectric Discontinuity on a Planar Waveguide", IEEE Trans. Microwave Theory and Techniques, Vol. MTT-23, pp. 193-198, February 1975.

20. M. Davarpanah, C. A. Goben and R. J. Bell, "Excitation Efficiency of Surface Electromagnetic Waves", to be published in Wave Electronics.

21. M. Davarpanah, C. A. Goben, D. L. Begley, and S. L. Griffith, "Measurement of Surface Electromagnetic Wave Coupling Efficiencies for Several Excitation Techniques", to be published in Applied Optics.

22. H. M. Barlow and J. Brown, Radio Surface Waves, New York, Oxford Press, 1962.

23. M. Davarpanah, "Excitation of Surface Electromagnetic Waves at Microwave Frequencies Using Optical Techniques", Ph.D. Dissertation, Univ. of Missouri-Rolla Library, Rolla, Mo., 1975.

24. G. Goubau, "Surface Waves and Their Application to Transmission Lines", J. Appl. Phys. Vol. 21, pp. 1119-1128, November 1950.

25. R. E. Collin, Field Theory of Guided Waves, New York: McGraw-Hill, 1960.

26. R. L. Gallawa et al., "The Surface Wave Transmission Line and Its Use in Communicating with High Speed Vehicles", IEEE Trans. Communication Technol., Vol. CT-17, pp. 518-524, October 1969.

27. B. Fisher, N. Marschall and H. J. Queisser, "Experimental Studies of Optical Surface Excitations", Surface Science, Vol. 34, pp. 50-61, January 1973.

28. A. Otto, "Excitation of Nonradiative Surface Plasma Waves in Silver by the Method of Frustrated Total Reflection", Zeitschrift fur Physik, Vol. 216, pp. 398-410, September 1968.

29. H. L. Bertoni, L. F. Felsen and J. W. Ra, "Evanescent Fields Produced by Total Reflection Beams", IEEE Trans. on Antennas and Propagation, Vol. AP-21, September 1973.

30. R. J. Bell, C. A. Goben, M. Davarpanah, K. Bhasin, D. L. Begley and A. C. Bauer, "Two-Dimensional Optics with Surface Electromagnetic Waves", Applied Optics, Vol. 14, pp. 1322-1325, June 1975.

31. R. J. Bell, M. Davarpanah, C. A. Goben, D. L. Begley, K. Bhasin and R. W. Alexander, Jr., "Measurements of Standing Waves and the Absorption Coefficients of Various Materials with Surface Electromagnetic Waves on Al", Applied Optics, Vol. 14, pp. 1579-1584, July 1975.

## REPORT OF INVENTIONS APPENDIX

This report presents the results of the first six months' work under contract DOT-TSC-1150 on determining the electrical characteristics of the Surface Electromagnetic Wave (SEW) vehicle coupler and the excitation of SEW on a steel rail.

After a diligent review, no innovation, discovery, improvement or invention was found.

110 copies

U. S. DEPARTMENT OF TRANSPORTATION
TRANSPORTATION SYSTEMS CENTER
KENDALL SQUARE, CAMBRIDGE, MA. 02142

OFFICIAL BUSINESS
PENALTY FOR PRIVATE USE, $300


POSTAGE AND FEES PAID
U. S. DEPARTMENT OF TRANSPORTATION
513